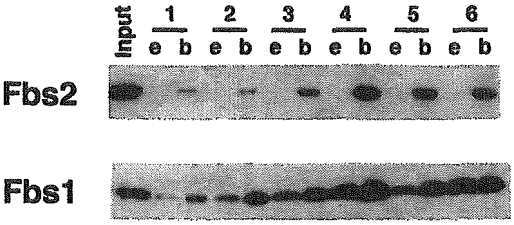

FIG. 4. **Pull-down analysis of the interaction of Fbs proteins with *N*-glycoproteins.** Extracts of cells expressing Fbs2 ΔF and Fbs1 ΔN-2 were incubated with glycoprotein-immobilized beads. The beads were washed, and then halves of the beads were eluted with *N,N'*-diacetylchitobiose (*e*), and the other halves were boiled with sample buffer (*b*). Lysates (7.5 μg), eluates, and bound proteins were analyzed by immunoblotting an anti-FLAG antibody (*top*) and their binding efficiencies were classified as −, ±, +, ++, and +++ (*bottom*).

Proteins (*N*-Glycan)	Fbs2		Fbs1	
	elute	bound	elute	bound
1. Fetuin (tri-antennary complex)	-	±	±	+
2. Asialo Fetuin (Gal-terminal tri-antennary)	-	±	+	++
3. GTF (GlcNAc-terminal tri-antennary)	-	+	+	++
4. Man-terminated Fetuin ($Man_3GlcNAc_2$)	-	++	+++	+++
5. Thyroglobulin ($Man_{7-9}GlcNAc_2$)	-	++	+	+++
6. RNaseB ($Man_{5-7}GlcNAc_2$)	-	++	++	+++

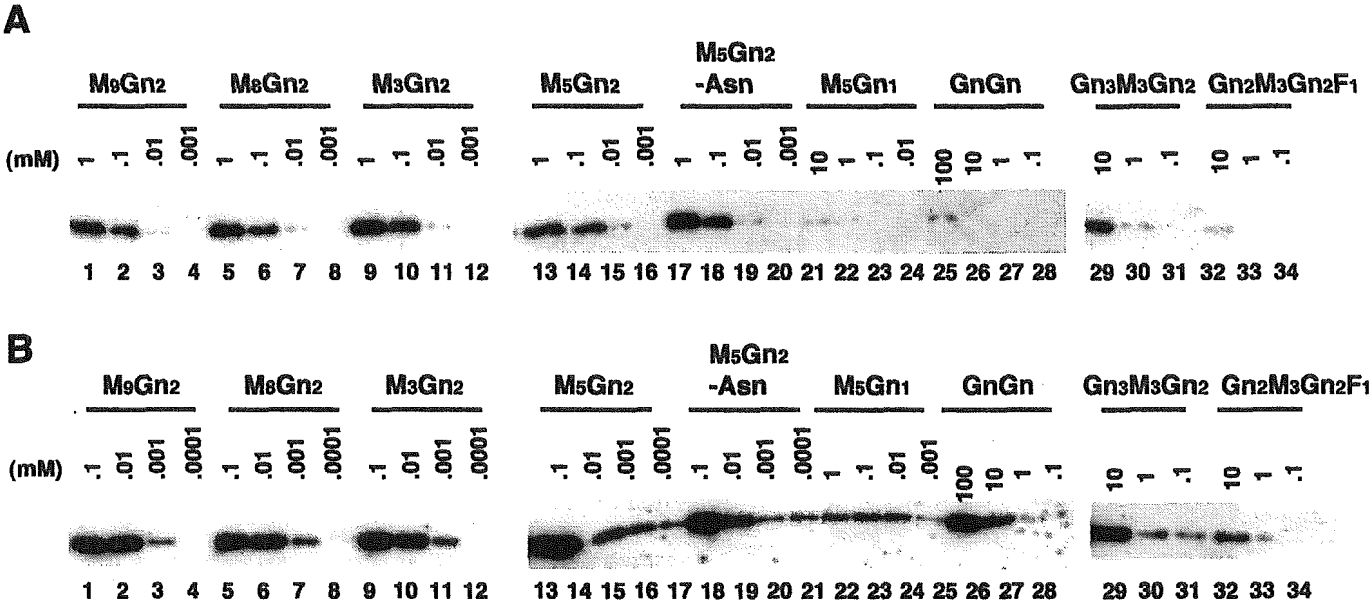

FIG. 5. **Elution of Fbs proteins bound to RNase-B immobilized beads with oligosaccharides.** After Fbs2 ΔF (*A*) or Fbs1 ΔN-2 (*B*) was retained on the RNase B immobilized beads, the bound Fbs protein was eluted by incubation with various concentrations of $Man_9GlcNAc_2$ (M_9Gn_2), $Man_8GlcNAc_2$ (M_8Gn_2), $Man_3GlcNAc_2$ (M_3Gn_2), $Man_5GlcNAc_2$ (M_5Gn_2), $Man_5GlcNAc_2$-asparagine (M_5Gn_2-*Asn*), $Man_5GlcNAc_1$ (M_5Gn_1), *N, N'*-diacetylchitobiose (*GnGn*), $GlcNAc_3Man_3GlcNAc_2$ ($Gn_3M_3Gn_2$), or $GlcNAc_2Man_3GlcNAc_2(Fuc)$ ($Gn_2M_3Gn_2F_1$). Note the differences in the concentrations of high mannose type oligosaccharides for elution between Fbs2 and Fbs1.

expression of Fbs1 is restricted to the brain and testis, the Fbs2 transcript is ubiquitously expressed in all tissues examined.

In Vitro Ubiquitylation Assay of Fbs2—To directly demonstrate the E3 ubiquitin ligase activity in SCF^{Fbs2}, we devised a fully reconstituted system for ubiquitylation of GTF in the presence of the NEDD8 system. To this end, we produced all components required for these systems as recombinant or purified proteins (see "Experimental Procedures"). Ubiquitylation of GTF by GST-tagged ubiquitin was detected by immunoblotting using an anti-fetuin or anti-GST antibody. No ubiquitylation activity was detected in the absence of E1, E2, ATP, SCF^{Fbs2}, or GTF (Fig. 3*A*). The amount of ubiquitylation increased in a time-dependent manner (Fig. 3*B*). In addition, *N*-glycanase F-treated fetuin (DGF) was not ubiquitylated *in vitro* by SCF^{Fbs2} (Fig. 3*B*). These results indicate that SCF^{Fbs2} is an E3 ubiquitin ligase that recognizes *N*-glycans in glycoproteins.

Binding Specificities of N-Glycans to Fbs1 and Fbs2—To compare the binding specificities to *N*-glycans between Fbs1 and Fbs2, a pull-down assay using several *N*-linked glycoproteins was carried out (Fig. 4). Whereas Fbs2 could bind to GTF but weakly to fetuin and asialofetuin, Fbs1 bound to asialofetuin and GTF more efficiently than to intact fetuin. Both Fbs1 and Fbs2 bound efficiently with glycoproteins containing mannose-terminated *N*-glycan(s), mannose-terminated fetuin, thyroglobulin, and RNase B, suggesting that mannose-terminated *N*-glycans (the number of mannose residues is irrelative) are required for the efficient binding of these Fbs proteins. On the other hand, the efficiency of elution of the proteins from the glycoproteins by chitobiose was different between Fbs1 and Fbs2. Although Fbs1 could be eluted efficiently by 0.1 M chitobiose from the *N*-linked glycoproteins tested, Fbs2 failed to be eluted by chitobiose. To characterize in more detail the binding specificities, we first quantified the oligosaccharide binding to Fbs proteins using a series of oligosaccharides labeled with 2-aminopyridine (25). However, we found that the innermost GlcNAc residue modified with 2-aminopyridine greatly reduced (10^{2-3}) the Fbs1 and Fbs2 binding (data not shown). Therefore, we next examined the efficiency of elution of the Fbs proteins

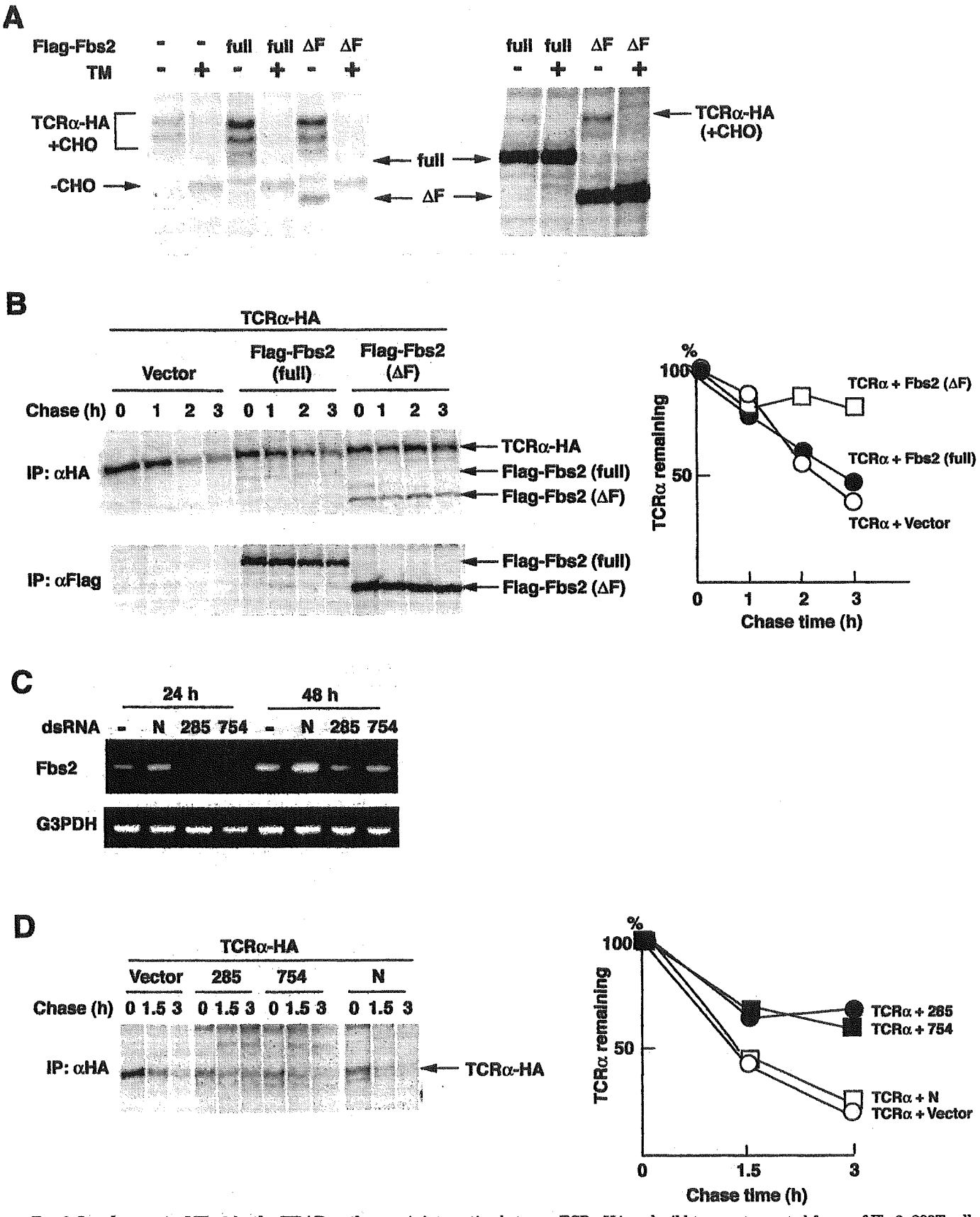

FIG. 6. **Involvement of Fbs2 in the ERAD pathway.** *A*, interaction between TCRα-HA and wild-type or truncated forms of Fbs2. 293T cells were transfected with TCRα-HA and/or various Fbs2 constructs. Twenty-four hours after transfection, cells were treated with (+) or without (−) 5 μg/ml tunicamycin (*TM*) for 2 h. Then, cells were labeled with [^{35}S]Met/Cys in the absence or presence of tunicamycin for 30 min. TCRα and Fbs2 derivatives were immunoprecipitated by anti-HA and anti-FLAG antibodies, respectively. *CHO*, carbohydrate oligosaccharide. *B*, effect of Fbs2 on the stability of TCRα. TCRα-HA was co-transfected with an empty vector (*Vector*), wild type (*full*), or FLAG-Fbs2 ΔF. 293T cells were pulse-labeled with [^{35}S]Met/Cys and chased for the indicated times. TCRα and Fbs2 derivatives were immunoprecipitated (*IP*) by anti-HA and anti-FLAG antibodies, respectively. The plotted data provide quantification analysis of the stability of TCRα over time. *C*, effect of nonspecific (*N*) or

from RNase B by several oligosaccharides (Fig. 5) (7). All *N*-glycans containing a diacetylchitobiose structure with mannose residues, $Man_9GlcNAc_2$, $Man_8GlcNAc_2$, $Man_5GlcNAc_2$, and $Man_3GlcNAc_2$ were found to cause elution of Fbs2 from RNase B at similar concentrations (Fig. 5*A*, *lanes 1–16*). In addition, the presence of the asparagine residue did not affect the efficiency of the elution (*lanes 13–20*). However, the amount of Fbs2 eluted by $Man_5GlcNAc_1$ or chitobiose was 3–4 orders of magnitude lower than that by $Man_{3-9}GlcNAc_2$, indicating that both the inner diacetylchitobiose structure and terminal mannose residues are required for efficient Fbs2 binding (compare *lanes 13–16* with *lanes 21–28*). The addition of GlcNAc residues on mannose residues in $Man_3GlcNAc_2$ reduced $\sim 10^2$ the elution efficiency, and core-fucosylation caused further reduction (*lanes 9–12* and *lanes 29–34*, Fig. 5*A*). The tendency of elution of Fbs1 bound to RNase B by oligosaccharides was similar to that of Fbs2 (Fig. 5*B*). Compared with Fbs2, however, all oligosaccharides tested were found to elute Fbs1 at almost 10^2 lower concentrations. These data suggest that $Man_{3-9}GlcNAc_2$ is required for the efficient binding of both Fbs1 and Fbs2 and that the dissociation of Fbs2 from the *N*-glycans is lower than that of Fbs1.

Involvement of Fbs2 in the ERAD Pathway—To investigate the role of Fbs2 in the ERAD pathway, we used the TCRα subunit as a substrate for ERAD. TCRα is a type I glycoprotein attached to four *N*-glycans, and unassembled TCRα chains are degraded by proteasomes following their dislocation from the ER membrane (26). To examine whether the interaction of Fbs2 with TCRα mediates *N*-glycans, TCRα-expressing cells were labeled in the presence of tunicamycin, a glycosylation inhibitor, and immunoprecipitated. After tunicamycin treatment, 38-kDa glycosylated TCRα-HA protein shifted to 28 kDa. Full-length Fbs2 and ΔF could interact with glycosylated TCRα, whereas they failed to interact with deglycosylated TCRα (Fig. 6*A*).

We performed pulse-chase analysis using 293T cells co-expressing HA-tagged TCRα (TCRα-HA) and FLAG-tagged Fbs2 derivatives (Fig. 6*B*). Although wild-type Fbs2 did not influence the kinetics of TCRα degradation, co-expression of ΔF efficiently suppressed the decay of TCRα (Fig. 6*B*). To confirm the involvement of Fbs2 in the ERAD pathway, we performed further experiments aimed at reducing the level of endogenous Fbs2 using synthetic siRNA (Fig. 6, *C* and *D*). Although a nonspecific control duplex (designated *N* in Fig. 6, *C* and *D*) did not affect the expression of Fbs2, Fbs2-specific siRNA (285 or 754) decreased the Fbs2 expression (Fig. 6*C*). In the pulse-chase analysis of TCRα, although reduction of TCRα expression still occurred with siRNAs both specific and nonspecific to Fbs2, only Fbs2-specific siRNAs, not the nonspecific ones, decreased the rate of TCRα degradation (Fig. 6*D*). These results point to the involvement of Fbs2 in the ERAD pathway for misfolded and unassembled glycoproteins through its interaction with *N*-glycans.

DISCUSSION

Most proteins in the secretory pathway, such as membrane proteins and secretory proteins, are modified with *N*-glycans in the ER. In the early secretory pathway, *N*-glycosylation facilitates conformational maturation by promoting the glycoprotein-folding machinery consisting of two homologous lectins, calnexin and calreticulin, which interact with monoglucosylated *N*-linked core glycans in concert with UDP-glucose:glycoprotein glucosyltransferase (UGGT) and glucosidase II (10, 27). Recent studies suggest that mannosidase I and EDEM, an ER-degradation-enhancing α-mannosidase-like lectin, play a pivotal role in the selective disposal of misfolded glycoproteins (14–16) and that the misfolded proteins are accepted from calnexin by EDEM (28, 29). In the present study, we report that Fbs2, in addition to Fbs1, formed an SCF-type ubiquitin ligase that is responsible for the ubiquitylation of *N*-linked glycoproteins in the ERAD pathway. These findings indicate that the *N*-glycan of misfolded proteins functions as a covalent tag for recognition by not only folding but also by degradation machinery.

Our data indicate that both Fbs1 and Fbs2 recognize *N*-linked high mannose oligosaccharides, especially their internal diacetylchitobiose structure. In many native glycoproteins, the internal diacetylchitobiose is not accessible to macromolecules such as peptide *N*-glycanase (PNGase), and cleavage of oligosaccharides requires denaturation of the glycoproteins *in vitro*. On the other hand, it has been suggested that UGGT, which is responsible for re-glucosylation of the substrate so that it can reassociate with calnexin or calreticulin in the ER, recognizes both the innermost GlcNAc unit of the oligosaccharide and protein domains with hydrophobic patches exposed in the substrates (30). As it is well known that re-glucosylation by UGGT occurs only if the glycoprotein is incompletely folded, UGGT serves as a sensor for misfolded proteins in the ER (27). Because Fbs proteins are involved in the ERAD pathway, the inner chitobiose residues of the target glycoproteins for Fbs may be exposed to outside molecules generated through protein denaturation. Thus, it is possible that Fbs proteins recognize inner chitobiose in a manner similar to peptide *N*-glycanase or UGGT.

We also found that Fbs2 as well as Fbs1 could recognize not only high mannose oligosaccharides but also other type *N*-glycans (Fig. 4), suggesting the general role of Fbs-related SCF in glycoprotein clearance in the cytosol. It is also possible that these ubiquitin ligases mediate ubiquitylation of exogenous or membrane proteins endocytosed, but leaked in the cytosol, into the cells. This is not unusual, because it is well known that extracellular proteins incorporated by phagocytosis into dendritic cells are presented to major histocompatibility complex class I molecules after proteasomal degradation (31). There are also other studies that demonstrate that the transfer of endocytosed proteins into the cytosol by unknown mechanisms prior to their proteasomal processing and/or destruction is sensitive to proteasome inhibitors (32).

Although Fbs proteins recognize high mannose *N*-glycans, their affinities for oligosaccharides seem to be different. An overlay assay for the glycoproteins using labeled Fbs proteins revealed that the strength of the binding ability of Fbs2 was weaker than that of Fbs1 (Fig. 1). Furthermore, using several oligosaccharides from *N*-linked glycoproteins, we showed that the dissociation of Fbs2 was lower than that of Fbs1 (Fig. 5). Although the *in vitro* ubiquitylation of GTF by SCF^{Fbs1} and the interaction of glycoproteins with Fbs1 in the overlay assay were inhibited by chitobiose, the addition of chitobiose inhibited neither ubiquitylation by SCF^{Fbs2} nor the interaction with

Fbs2-specific siRNAs (siRNA$^{285-304}$ and siRNA$^{754-773}$, here named simply *285* and *754*, respectively) on the relative level of the Fbs2 transcript in 293T cells. mRNAs prepared from cells were converted to cDNAs, and then the same amount of each cDNA (as estimated with 25 cycles of PCR for the glyceroaldehyde-3-phosphate dehydrogenase (*G3PDH*) gene) was subjected to 35 cycles of PCR. *D*, effect of siRNA-Fbs2 on the stability of TCRα. TCRα-HA was co-transfected with an empty vector (*Vector*), 60 nM siRNA directed against Fbs2 (*285* and *754*), or 60 nM nonspecific siRNA (*N*). 293T cells were pulse-labeled with [^{35}S]Met/Cys and chased for the indicated times. The relative intensities were quantified as the plotted data to show the stability of TCRα over time.

Fbs2 (data not shown). In addition, whereas Fbs1 interacted strongly with pre-integrin β1 (7), Fbs2 did so only weakly (data not shown). On the other hand, Fbs2 bound strongly to TCRα, relative to Fbs1, in 293T cells, and the degradation of TCRα was more markedly suppressed by the dominant negative form of Fbs2 than by that of Fbs1 (Fig. 6, and data not shown). In addition to these properties, the Fbs2 transcript is widely expressed in various tissues in contrast to the limited expression of Fbs1 in the brain and testis (Fig. 2), suggesting that these Fbs proteins have distinct substrates or roles *in vivo*.

It has been reported that Fbs1 belongs to a subfamily consisting of at least five homologous F-box proteins (23). Among them, the FBG3 protein exhibits 75% identity with Fbs2, and the identity of Fbs1 and Fbs2 is similar to that of Fbs1 and FBG3 (23). Interestingly, *Fbs1*, *FBG3*, and *Fbs2* genes are located in tandem on chromosome (23), and the expression of FBG3 is observed ubiquitously but strongly in the brain and testis (data not shown). It is anticipated that FBG3 can recognize high mannose *N*-glycans because of their high homology. However, we could not detect any sugar-binding activity for FBG3 even though several assay systems were used in our studies. One possibility is that FBG3 suffers a negative modification that prevents it from accessing glycoproteins or that some modification of FBG3 is needed for the target recognition. Alternatively, this could be simply due to different substrate specificities. On the other hand, the expression of FBG4/Fbx17 and FBG5 transcripts is restricted, compared with those of Fbs2 and FBG3 (23), and the FBG4 protein shows a high homology with FBG5 (23), suggesting that they are another subfamily of F-box proteins that recognizes other sugar chains or other modifications.

Acknowledgments—We thank Y. Ito and R. R. Kopito for providing $Man_9GlcNAc_2$ and the TCRα-HA expression plasmid, respectively.

REFERENCES

1. Hershko, A., and Ciechanover, A. (1998) *Annu. Rev. Biochem.* **67,** 425–479
2. Deshaies, R. J. (1999) *Annu. Rev. Cell Dev. Biol.* **15,** 435–467
3. Winston, J. T., Koepp, D. M., Zhu, C., Elledge, S. J., and Harper, J. W. (1999) *Curr. Biol.* **9,** 1180–1182
4. Kipreos, E. T., and Pagano, M. (2000) *Genome. Biol.* **1,** 3002.1–3002.7
5. Ivan, M., Kondo, K., Yang, H., Kim, W., Valiando, J., Ohh, M., Salic, A., Asara, J. M., Lane, W. S., and Kaelin, W. G., Jr. (2001) *Science* **292,** 464–468
6. Jaakkola, P., Mole, D. R., Tian, Y. M., Wilson, M. I., Gielbert, J., Gaskell, S. J., Kriegsheim, A., Hebestreit, H. F., Mukherji, M., Schofield, C. J., Maxwell, P. H., Pugh, C. W., and Ratcliffe, P. J. (2001) *Science* **292,** 468–472
7. Yoshida, Y., Chiba, T., Tokunaga, F., Kawasaki, H., Iwai, K., Suzuki, T., Ito, Y., Matsuoka, K., Yoshida, M., Tanaka, K., and Tai, T. (2002) *Nature* **418,** 438–442
8. Fiedler, K., and Simons, K. (1995) *Cell* **81,** 309–312
9. Ellgaard, L., Molinari, M., and Helenius, A. (1999) *Science* **286,** 1882–1888
10. Helenius, A., and Aebi, M. (2001) *Science* **291,** 2364–2369
11. Plemper, R. K., and Wolf, D. H. (1999) *Trends Biochem. Sci.* **24,** 266–270
12. Brodsky, J. L., and McCracken, A. A. (1999) *Semin. Cell Dev. Biol.* **10,** 507–513
13. Tsai, B., Ye, Y., and Rapoport, T. A. (2002) *Nat. Rev. Mol. Cell Biol.* **3,** 246–255
14. Hosokawa, N., Wada, I., Hasegawa, K., Yorihuzi, T., Tremblay, L. O., Herscovics, A., and Nagata, K. (2001) *EMBO Rep.* **2,** 415–422
15. Jakob, C. A., Bodmer, D., Spirig, U., Battig, P., Marcil, A., Dignard, D., Bergeron, J. J., Thomas, D. Y., and Aebi, M. (2001) *EMBO Rep.* **2,** 423–430
16. Nakatsukasa, K., Nishikawa, S., Hosokawa, N., Nagata, K., and Endo, T. (2001) *J. Biol. Chem.* **276,** 8635–8638
17. Bays, N. W., Gardner, R. G., Seelig, L. P., Joazeiro, C. A., and Hampton, R. Y. (2001) *Nat. Cell Biol.* **3,** 24–29
18. Swanson, R., Locher, M., and Hochstrasser, M. (2001) *Genes Dev.* **15,** 2660–2674
19. Fang, D., Haraguchi, Y., Jinno, A., Soda, Y., Shimizu, N., and Hoshino, H. (1999) *Biochem. Biophys. Res. Commun.* **261,** 357–363
20. Meacham, G. C., Patterson, C., Zhang, W., Younger, J. M., and Cyr, D. M. (2001) *Nat. Cell Biol.* **3,** 100–105
21. Imai, Y., Soda, M., Inoue, H., Hattori, N., Mizuno, Y., and Takahashi, R. (2001) *Cell* **105,** 891–902
22. Erhardt, J. A., Hynicka, W., DiBenedetto, A., Shen, N., Stone, N., Paulson, H., and Pittman, R. N. (1998) *J. Biol. Chem.* **273,** 35222–35227
23. Ilyin, G. P., Serandour, A. L., Pigeon, C., Rialland, M., Glaise, D., and Guguen-Guillouzo, C. (2002) *Gene* **296,** 11–20
24. Kawakami, T., Chiba, T., Suzuki, T., Iwai, K., Yamanaka, K., Minato, N., Suzuki, H., Shimbara, N., Hidaka, Y., Osaka, F., Omata, M., and Tanaka, K. (2001) *EMBO J.* **20,** 4003–4012
25. Hase, S., Natsuka, S., Oku, H., and Ikenaka, T. (1987) *Anal. Biochem.* **167,** 321–326
26. Yu, H., Kaung, G., Kobayashi, S., and Kopito, R. R. (1997) *J. Biol. Chem.* **272,** 20800–20804
27. Parodi, A. J. (2000) *Annu. Rev. Biochem.* **69,** 69–93
28. Oda, Y., Hosokawa, N., Wada, I., and Nagata, K. (2003) *Science* **299,** 1394–1397
29. Molinari, M., Calanca, V., Galli, C., Lucca, P., and Paganetti, P. (2003) *Science* **299,** 1397–1400
30. Sousa, M., and Parodi, A. J. (1995) *EMBO J.* **14,** 4196–4203
31. Castellino, F., Boucher, P. E., Eichelberg, K., Mayhew, M., Rothman, J. E., Houghton, A. N., and Germain, R. N. (2000) *J. Exp. Med.* **191,** 1957–1964
32. Kovacsovics-Bankowski, M., and Rock, K. L. (1995) *Science* **267,** 243–246

The EMBO Journal Vol. 22 No. 14 pp. 3557–3567, 2003

The molecular chaperone Hsp90 plays a role in the assembly and maintenance of the 26S proteasome

Jun Imai[1,2,3], Mikako Maruya[2,3], Hideki Yashiroda[1,3], Ichiro Yahara[3,4] and Keiji Tanaka[1,3,5]

[1]Department of Molecular Oncology and [2]Department of Cell Biology, Tokyo Metropolitan Institute of Medical Science, Honkomagome 3-18-22, Bunkyo-ku, Tokyo 113-8613, [3]CREST, Japan Science and Technology Corporation, Honmachi 4-1-8, Kawaguchi, Saitama 332-0012 and [4]Ina Laboratory, Medical and Biological Laboratories Co. Ltd, 1063-103 Ohara Terasawaoka, Ina, Nagano 396-0002, Japan

[5]Corresponding author
e-mail: tanakak@rinshoken.or.jp

Hsp90 has a diverse array of cellular roles including protein folding, stress response and signal transduction. Herein we report a novel function for Hsp90 in the ATP-dependent assembly of the 26S proteasome. Functional loss of Hsp90 using a temperature-sensitive mutant in yeast caused dissociation of the 26S proteasome. Conversely, these dissociated constituents reassembled in Hsp90-dependent fashion both *in vivo* and *in vitro*; the process required ATP-hydrolysis and was suppressed by the Hsp90 inhibitor geldanamycin. We also found genetic interactions between Hsp90 and several proteasomal Rpn (Regulatory particle non-ATPase subunit) genes, emphasizing the importance of Hsp90 to the integrity of the 26S proteasome. Our results indicate that Hsp90 interacts with the 26S proteasome and plays a principal role in the assembly and maintenance of the 26S proteasome.

Keywords: assembly/Hsp90/maintenance/26S proteasome/yeast

Introduction

The high density of protein molecules in the cytosol increases the likelihood that partially folded or unfolded proteins will undergo off-pathway reactions, such as aggregation, in the protein biosynthetic pathway or by postsynthesis damage. Molecular chaperones recognize proteins with non-native structures, prevent them from irreversible aggregation and assist in their conversion to a functional conformation (Frydman, 2001). On the other hand, the ubiquitin–proteasome pathway plays a pivotal role in selective destruction of misfolded and unassembled proteins (Sherman and Goldberg, 2001). Since chaperones and proteasomes appear to recognize common substrates under non-native states, these two pathways act jointly to prevent aggregation and accumulation of abnormal proteins, thus maintaining protein homeostasis in cells. However, the relationship between molecular chaperones and the ubiquitin–proteasome system is still largely unknown.

Most cellular proteins in eukaryotic cells are targeted for degradation by the 26S proteasome, usually after they have been covalently attached to ubiquitin in the form of a poly-ubiquitin chain functioning as a degradation signal (Pickart, 2001). The 26S proteasome, a eukaryotic ATP-dependent protease, is composed of a catalytic 20S proteasome (alias CP, core particle) and a pair of symmetrically disposed regulatory particles (RP, alias PA700 or the 19S complex) (Baumeister *et al.*, 1998). RP is attached to both ends of the central CP in opposite orientation to form the active 26S proteasome. The 26S proteasome with a molecular mass of ~2.5 MDa acts as a highly organized apparatus for proteolysis. The 20S proteasome is composed of two copies of 14 different subunits, seven distinct α-type and seven distinct β-type subunits. It is a barrel-like particle formed by the axial stacking of four rings made up of two outer α-rings and two inner β-rings, associated in the order αββα. Three β-type subunits of each inner ring have catalytically active threonine residues at their N-termini, and these active sites reside in a chamber formed by the centers of the abutting β-rings. The regulator RP is a protein complex (>700 kDa) composed of ~20 subunits, each 25–110 kDa in size (Baumeister *et al.*, 1998). RP consists of two subcomplexes, known as 'base' and 'lid', which, in the 26S proteasome, correspond to the portions of RP proximal and distal, respectively, to the 20S proteasome (Glickman *et al.*, 1998). The base is mainly composed of up to six ATPases (Rpt, Regulatory particle triple ATPase), while the lid contains multiple non-ATPase subunits (Rpn). The metabolic energy liberated by these Rpt functions is probably utilized for unfolding target proteins so that they can penetrate the channel of the α- and β-rings of the 20S proteasome. However, the roles of many other RP subunits remain undefined.

Of many molecular chaperones, Hsp90 is one of the major species which also requires ATP for its *in vivo* functions (Panaretou *et al.*,1998; Young *et al.*, 2001). It is among the most abundant proteins in cells, occupying ~1–2% of total cellular proteins (Frydman, 2001). The major role of Hsp90 is to manage protein folding, but it also plays a critical role in signal transduction pathways that include mainly steroid receptors and protein kinases (Richter and Buchner, 2001). In *Saccharomyces cerevisiae*, two Hsp90 species with redundant functions, named Hsp82 and Hsc82, are present, which are equivalent to mammalian Hsp90α and Hsp90β, respectively.

In the present study of Hsp90 in the budding yeast, we unexpectedly noticed that *in vivo* inactivation of Hsp90 using the temperature-sensitive (ts⁻) *hsp82–4Δhsc82* mutant cells (Kimura *et al.*, 1994) caused almost complete dissociation of the 26S proteasome into its constituents. Furthermore, we found that Hsp90 contributes not only to maintain the functional integrity of the 26S proteasome but

also to assist its assembly *in vivo* and *in vitro* in an ATP-dependent manner. In addition, we also provide the genetic evidence of *in vivo* linkage between Hsp90 and the 26S proteasome. Thus the participation of Hsp90 in the 26S proteasome assembly may provide new mechanistic insight into the cooperative interactions between molecular chaperones and proteolysis systems.

Results

Severe thermal stress causes disassembly of the 26S proteasome

To focus on the relationship between stress response and the cellular proteolysis machinery, we examined the effect of severe heat stress on the functional state of the proteasome, which is subclassified into three species in the budding yeast; i.e. the free 20S proteasome (alias CP and here designated simply as C) and RP associated with both sides of CP (R2C) or one side of CP (RC), as described by Glickman *et al.* (1998). Wild-type (WT) cells grown at 25°C were first incubated at 37°C for 1 h. This step was essential to allow the cells to survive a subsequent severe thermal insult. The same cells were incubated at 50°C for 20 min and then shifted to normal culture conditions at 25°C. Upon these stresses, after preconditioning at 37°C, more than 80% of the cells were viable, forming colonies when plated at 25°C (Imai and Yahara, 2000).

Native (non-denaturing) polyacrylamide gel electrophoresis (PAGE) analysis and subsequent western blotting using antibodies against the yeast 20S proteasome

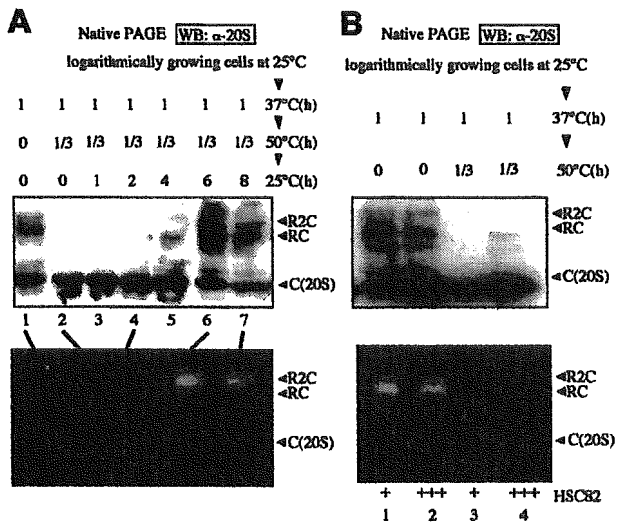

Fig. 1. Dissociation and reassembly of the 26S proteasome after severe heat shock. (A) Crude extracts (5 μg) of cells thermally treated as indicated were subjected to native PAGE followed by western blotting (WB) with anti-20S proteasome (top). Cell extracts (20 μg, top, lanes 1, 2, 4, 6 and 7) were loaded onto native PAGE, and thereafter Suc-LLVY-AMC degrading activities were assayed by the in-gel overlay method with 2 mM ATP (bottom). See text for explanation of symbols R2C, RC and C (20S). (B) Effect of overexpression (designated as +++) of Hsc82 on the disassembly of the 26S proteasome by severe heat shock. The analyses were similar to those described in (A), except that cells were grown in SC-U medium and cell extracts were prepared from control cells (YPH500/pYO326, lanes 1 and 3) and Hsc82 overexpressing cells (YPH500/pYO326-HSC82, lanes 2 and 4). Note that the magnitude of the increased level by a plasmid overexpressing Hsp82 was more than 5-fold (Imai and Yahara, 2000).

revealed a marked decrease of both the R2C and RC forms of the 26S proteasome after severe heat shock at 50°C, and a considerable increase in the amount of free 20S proteasome (Figure 1A, lanes 2–4). When these heat-shocked cells were reversed to culture at 25°C, it took ~6 h for the full recovery of the 26S proteasome (Figure 1A, lane 6). We also examined the peptidase activity of the 26S proteasome by the in-gel overlay assay. Samples of cell extracts were subjected to native PAGE, and peptide-degrading activity was detected by soaking the gel in a solution containing the fluorogenic peptide succinyl-Leu-Leu-Val-Tyr-7-amino-4-methylcoumarin (Suc-LLVY-AMC). As shown in Figure 1A (bottom), the dissociated 20S proteasome due to severe thermal insults was the latent form and the reassembled 26S proteasome (after incubation at 25°C) was functionally active.

In addition, we found that overexpression of Hsp90 (Hsc82) partially suppressed the destruction of the 26S proteasome caused by severe thermal insult, as detected by western blot and in-gel overlay analyses (Figure 1B). On the other hand, overexpression of Hsp70 (Ssa1) had no appreciable protective effect on the proteasome disassembly (data not shown).

Disassembly of the 26S proteasome caused by inactivation of Hsp90

In the next step, we examined the mechanism through which Hsp90 protects against disassembly of the 26S proteasome by severe thermal stress. For this purpose, we analyzed the structure of the 26S proteasome under defective conditions of Hsp90 using temperature-sensitive (ts^-) *hsp82–4Δhsc82* cells (YOK5) (hereafter, the mutant yeast is simply described as *hsp82-4* cells). First, we examined the 26S proteasome by the in-gel peptidase assay. As shown in Figure 2A (top), two slowly migrating active proteasomes, corresponding to R2C and RC, were evident in extracts of WT cells irrespective of the culture temperature (25 or 37°C). However, the signals corresponding to positions of R2C and RC markedly decreased when only samples prepared from *hsp82-4* cells that had been cultured for 8 h at non-permissive temperature of 37°C were used (Figure 2A). Activities similar to those of WT cell extracts were observed when extracts of *hsp82-4* cells cultured at permissive temperature were used. Moreover, the addition of SDS, which activates the latent 20S proteasome *in vitro*, caused marked activation of the 20S proteasome, and the magnitude of activation was augmented when we used the crude extracts of *hsp82-4* cells that had been cultured for 8 h at 37°C (Figure 2A, bottom). These results indicate that inactivation of Hsp90 causes dissociation of the active 26S proteasome into its constituents containing the 20S proteasome.

To confirm these observations, we loaded the samples prepared from WT and *hsp82-4* cells, which had been incubated for various times under a non-permissive temperature, onto native PAGE and SDS–PAGE, and then conducted western blotting with anti-20S proteasome. In the native PAGE, the three species of the proteasome, i.e. R2C, RC and C, were evident in WT cells even after 8 h incubation (Figure 2B, bottom). In contrast, destruction of both bands with lower electrophoretic mobility, corresponding to the R2C and RC forms of the 26S proteasome, began within only 4 h of inactivation of Hsp90, though it

took 8 h for their complete loss in *hsp82-4* cells. Consequently, loss of Hsp90 was associated with an increase in free 20S proteasome. However, the total amounts of the 20S proteasome analyzed by western blotting after SDS–PAGE, detected as several bands ranging from 20 to 35 kDa, remained unchanged. Thus it is clear that loss of function of Hsp90 causes dissociation of the 26S proteasome into its constituents, including the 20S proteasome. We then compared peptidase activities of the proteasome and cell viability under the same conditions. Both values were unchanged in WT cells, but the peptidase activities gradually decreased after around 4 h incubation at 37°C and almost completely disappeared upon incubation for 8 h in *hsp82-4* cells (Figure 2B, top). It was noteworthy that in these cells, the R2C form disappeared before the RC form and the activities of the proteasome were decreased (4 h after the shift), followed by the loss of the RC form (Figure 2B, top and bottom). Importantly, the loss of proteasome activities in *hsp82-4* cells occurred faster than cell death, indicating that the structural abnormality of the 26S proteasome is not due to cell death.

When the same electrophoretic and immunoblotting analyses were conducted using anti-Rpt1 (Figure 2C, left) and anti-Rpn12 (Figure 2D, left), the former is an ATPase base subunit and the latter is a non-ATPase lid subunit of RP (Glickman *et al.*, 1998), two slowly migrating R2C and RC bands were evident in native PAGE in all cases, except *hsp82-4* cells, under non-permissive temperature. Again, comparable amounts of Rpt1 and Rpn12 subunits of the RP complex were detected even under culture at 37°C by SDS–PAGE (see bottom panels). Intriguingly, excess loading of samples revealed the presence of Rpn12 and Rpn9, another lid subunit, at rapidly migrating positions, but their electrophoretic mobilities differed from each other (Figure 2E), indicating dissociation of the lid complex under defective Hsp90 conditions of the cells.

We also confirmed the involvement of Hsp90 in the maintenance of the 26S proteasome by shutting off Hsp82 expression using *GAL1* promoter. Repression of Hsp82 expression by replacement of galactose with glucose in the media resulted in the disappearance of the 26S proteasome (Figure 2C, right). Moreover, we observed that geldanamycin (GA), an Hsp90 inhibitor, caused loss of the 26S proteasome in *hsp82-4* cells even under permissive temperature, although it had no appreciable effects on the proteasomal states in WT cells (Figure 2D, right). These results strongly suggest that Hsp90 is essential for the 26S proteasome. Curiously, we repeatedly observed the sensitivity of *hsp82-4*, but not WT cells, to GA in both *in vivo* (Figures 2 and 3) and *in vitro* (Figure 4) analyses. The exact reason is unclear, but GA may be easily accessible to the active ATPase site of the *hsp82-4* protein, perhaps because of its abnormal conformation.

Hsp90-dependent in vivo assembly of the 26S proteasome

We first tested the physical interaction between Hsp90 and the 26S proteasome *in vivo*. For this purpose, we purified the 26S proteasome in a single step, using a Ni^+-resin column, from extracts of WT (J106) and *hsp82-4* cells (YOK5RH), whose *RPT1* was replaced by *6×His-RPT1*. The subunit composition of the enzyme from WT cells resembled that from *hsp82-4* cells grown at 25°C (data not shown). In both preparations, the addition of MG132 almost completely inhibited the hydrolysis activity of Suc-LLVY-AMC, revealing no contamination of other protease(s), and the specific activity of the purified 26S proteasome resulted in >10-fold increase in Suc-LLVY-AMC hydrolysis (data not shown). Intriguingly, compared with that WT cells, considerable amounts of Hsp82 were associated with affinity-purified 26S proteasome and larger amounts of Hsp90 were associated with the 26S proteasome from *hsp82-4* cells, as judged by the similar contents of various proteasomal subunits (Figure 3A, left), though the total Hsp90 contents in *hsp82-4* cell extracts were much less than those of the WT extracts because of the lack of Hsc82 in *hsp82-4* cells. Native PAGE and immunoblotting using anti-Hsp82 against Hsp82-depleted cells revealed that anti-Hsp82 reacted strongly with the R2C form than with RC form, but not appreciably with CP, indicating that Hsp82 associates with the 26S proteasome through the RP complex (Figure 3A, right). Intriguingly, even when the amounts of Hsp82 decreased to ~one-tenth of WT, Hsp82 only bound to R2C and RC (Figure 3A, right), indicating a high affinity of Hsp90 with the 26S proteasome.

We next examined the role of Hsp90 in the *in vivo* assembly of the 26S proteasome. When both WT and *hsp82-4* cells were grown at 25°C, the Suc-LLVY-AMC degrading activity of the 26S proteasome affinity-purified from the same amounts of crude cell extracts was almost similar, even when the peptidase assay was carried out at 37°C in the presence of ATP (time zero in Figure 3B, blue line). However, when *hsp82-4* cells were cultured for 8 h after a shift to 37°C, no appreciable amounts of proteasomal proteins were recovered by purifying operation using the same Ni^+-resin column, and consequently very little Suc-LLVY-AMC degrading activity was observed in the peptidase assay (data not shown). These results again indicated loss of the 26S proteasome under Hsp90-defective conditions of the cells.

In the next experiments, we examined whether, once disassembled, the proteasome in *hsp82-4* cells cultured under a non-permissive temperature could reassemble when the same Hsp90-inactivated cells were shifted to permissive temperature of 25°C. After heat shock at 37°C for 6 h, we added cycloheximide (CHX) to inhibit *de novo* protein synthesis (time zero in Figure 3B) and then these cells were shifted to 25°C for further culture. The 26S proteasome was affinity-purified from the same amount of cell extracts after reculture for the indicated time intervals. As shown in Figure 3B (right), 2 h after shifting to 25°C a considerable Suc-LLVY-AMC degrading activity was restored (black line). Of note, this restoration was independent of the newly synthesized proteasome because of the presence of CHX, suggesting the reassembly of the 26S proteasome subsequent to the functional recovery of Hsp90. Interestingly, this reactivation was diminished in GA-treated *hsp82-4* cells at the time of shift to 25°C and then was maintained at 25°C (red line), indicating that the ATPase function of Hsp90 is necessary for the restoration of the 26S proteasome. In contrast, continued culture in non-permissive temperature at 37°C was not associated with such increment in proteasomal peptidase activity (green line). In parallel analyses using WT cells

(Figure 3B, left), irrespective of heat shock, and *hsp82-4* cells under permissive temperature (Figure 3B, right, blue line), the Suc-LLVY-AMC degrading activities gradually diminished after addition of CHX. These results suggested that the restoration of peptidase activity is linked to the proper assembly of the 26S proteasome, assuming that the

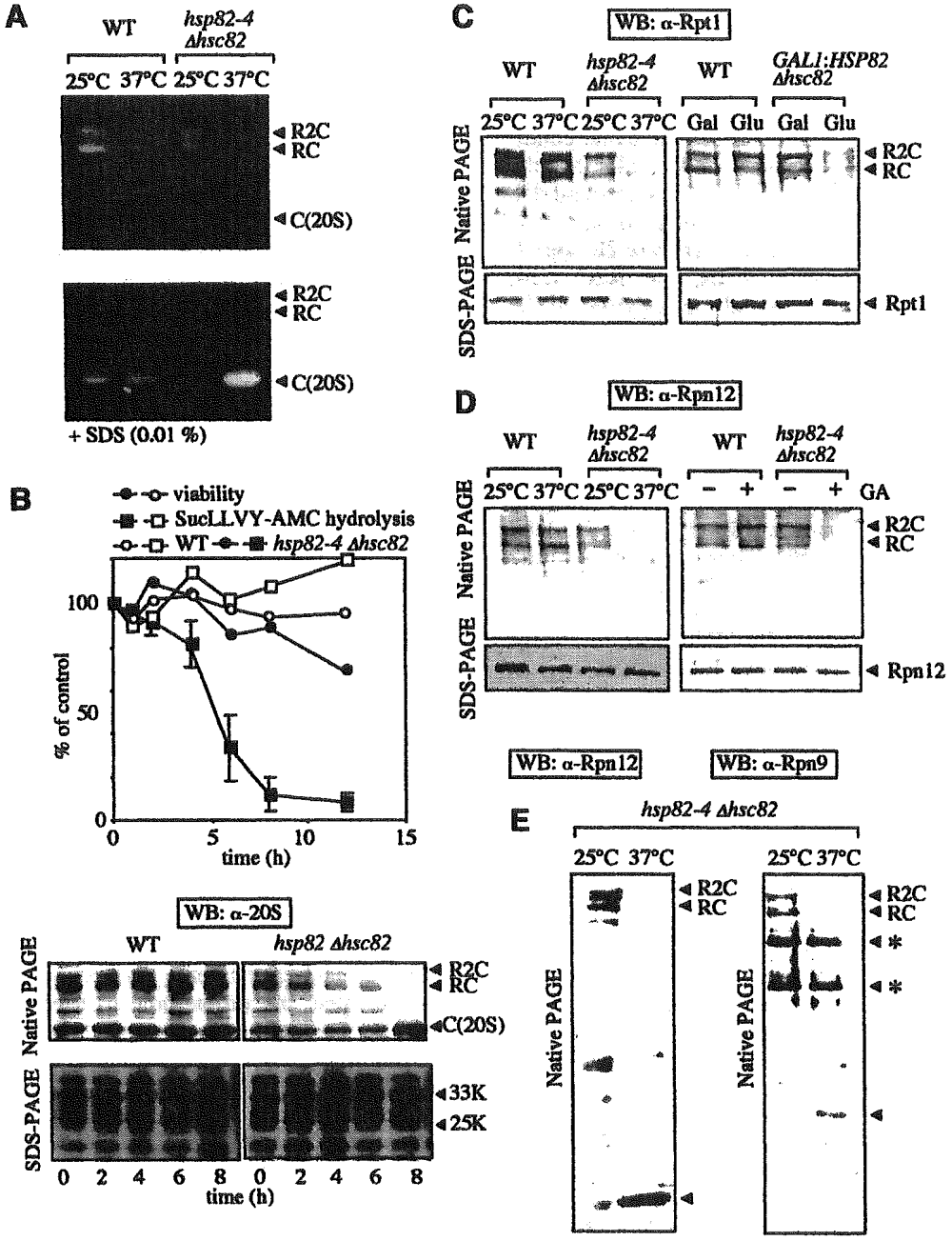

Fig. 2. Electrophoretic analyses of the 26S proteasome in *hsp82-4* cells. (**A**) In-gel overlay assay of peptidase activity of the proteasome separated by native PAGE. WT cells (YPH500) and *hsp82–4Δhsc82* cells (YOK5H) grown at 25°C were shifted at 37°C and maintained for another 8 h or continued culturing at 25°C. These cell extracts (20 μg) were analyzed as in Figure 1 in the presence of 2 mM ATP (top) or 0.01% SDS (bottom). (**B**) WT and *hsp82-4* cells grown at 25°C were shifted to 37°C and maintained for various times up to 12 h. Cells were sampled at each time point and then cell viability and Suc-LLVY-AMC degrading activity of the 26S proteasome affinity-purified were measured (top). The results are expressed relative to the result at time zero in WT cells. Open and closed squares represent activities of the 26S proteasome from WT and *hsp82-4* cells, respectively. Open and filled circles represent viability of WT and *hsp82-4* cells, respectively. Identical amounts of cell extracts were loaded onto native PAGE (top, 5 μg) and SDS–PAGE (bottom, 1 μg), followed by immunoblotting with anti-20S proteasome (bottom). (**C**) Western blotting with anti-Rpt1. The analyses were the same as for (B), except that anti-Rpt1 and 1 μg protein were used for native PAGE (left). The WT and *GAL1:HSP82 Δhsc82* cells (5CG2) grown at 30°C in YPGal were transferred to YPD and maintained for another 12 h or continued culturing in YPGal (right). The analyses were the same as for the left panel. (**D**) Western blotting with anti-Rpn12. The analyses were the same as for (B), except that anti-Rpn12 was used (left) and WT and *hsp82-4* cells grown at 25°C were treated (+) or mock treated (–) with GA (18 μM) followed by further culture at 25°C for 3 h (right). (**E**) Excess loading analyses. The same cell extracts in (D) for *hsp82-4* cells were analyzed by native PAGE and western blotting with anti-Rpn12 (left), except that 10 μg protein (lanes 1 and 2) was used. The same analysis was conducted using anti-Rpn9 and 10 μg protein (lanes 3 and 4). The band, indicated by arrowheads in both panels, was specific for antibodies against Rpn9 and Rpn12, respectively. Asterisks in the right panel indicate non-specific bands for anti-Rpn9.

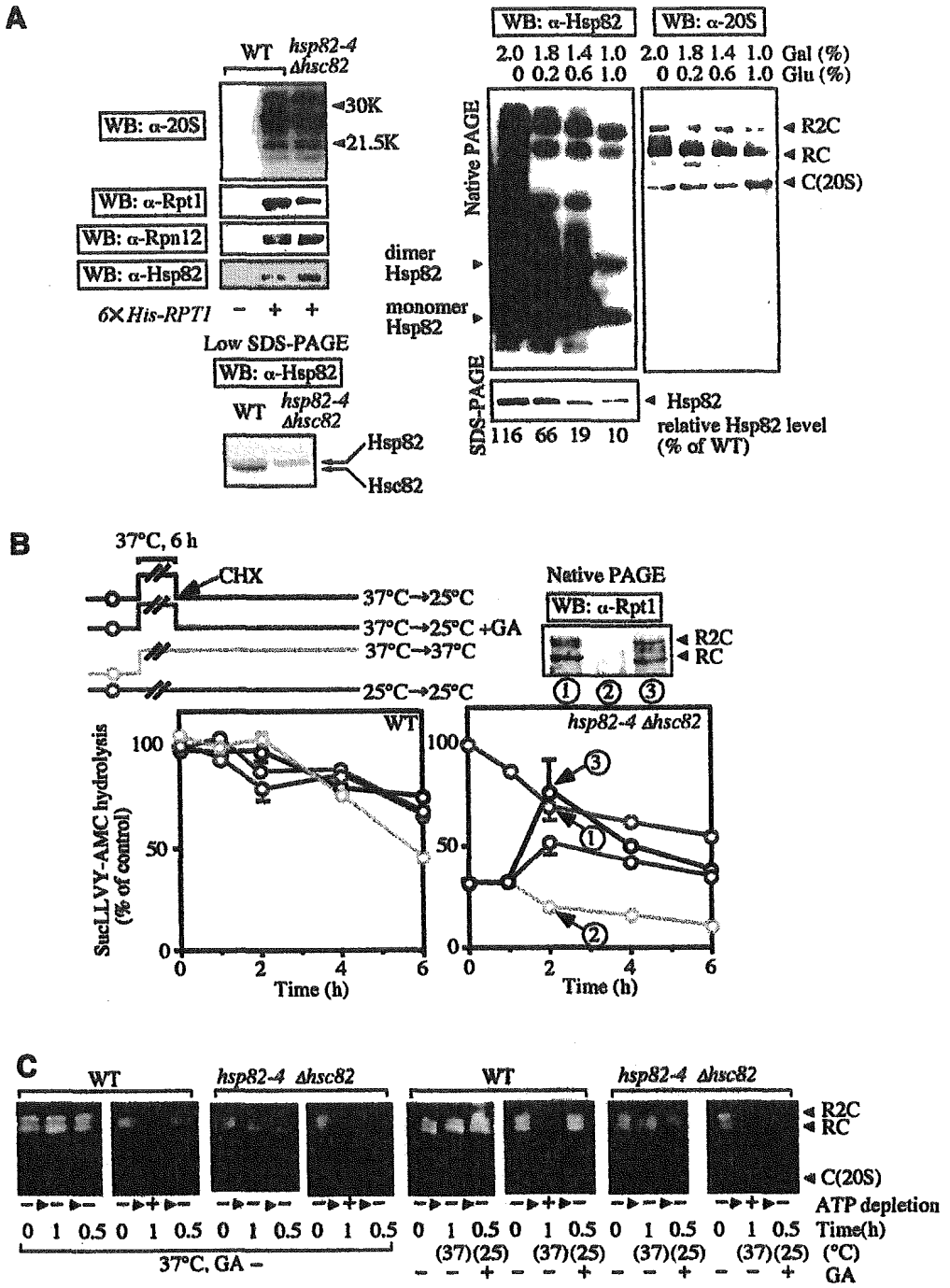

Fig. 3. *In vivo* analyses of the 26S proteasome under conditions with or without Hsp90 inactivation. (A) Western blotting was carried out with anti-Hsp82 and various proteasomal antibodies for the 26S proteasome (100 ng, left) affinity-purified from the extracts of WT (J106) and *hsp82–4Δhsc82* cells (YOK5RH) grown at 25°C by a Ni^{+}-resin column (–, YPH500, WT cells without *6×His-RPT1*). Western blotting after unconventional (low) SDS–PAGE (Imai and Yahara, 2000) was conducted to differentiate between Hsc82 and Hsp82 in the crude extracts (1 μg, left). Note that anti-Hsp82 reacted in a fashion similar to Hsc82 and Hsp82. Western blotting with anti-Hsp82 and anti-20S proteasome was carried out for Hsp82-depleted cells (5CG2) whose Hsp90 levels were varied by culturing with different combinations of Gal and Glu (right). The same amounts of cell extracts were loaded onto native PAGE (top, 5 μg) and SDS–PAGE (bottom, 1 μg), followed by immunoblotting with anti-Hsp82 and anti-20S proteasome. (**B**) WT (left) and *hsp82-4* cells (right) grown at 25°C were shifted to 37°C and maintained for an additional 6 h. At time zero, cells were shifted to the indicated temperatures followed by the addition of cycloheximide (CHX, 100 μg/ml). Cells were sampled at each time point and the Suc-LLVY-AMC degrading activity of the 26S proteasome affinity-purified as in (A) was measured. The activities are expressed relative to the activity at time zero in WT cells grown at 25°C. Blue lines, cells grown at 25°C throughout the experimental period; black lines, cells grown at 25°C were shifted to 37°C for 6 h and then to 25°C at time zero; red lines, similar to black lines except that the cells were treated with GA (18 μM) at time zero; green lines, cells grown at 25°C were shifted to 37°C for 6 h and further incubated at 37°C after time zero. Crude extracts (1 μg) of *hsp82-4* cells from positions denoted 1, 2 and 3 (right bottom) were separated by native PAGE and analyzed by western blotting with anti-Rpt1 (right top). Data are means ± SEM. (**C**) ATP requirement for Hsp90-dependent 26S proteasome assembly. WT and *hsp82-4* cells grown at 25°C were metabolically poisoned with 10 mM deoxyglucose and 10 mM sodium azide for 1 h at 37°C (designated + for ATP depletion). Cells cultured with YPD media without ATP-depletion are marked –. Thereafter, cells were shifted to YPD media for 30 min at 37°C (left panels) or YPD media containing GA (18 μM) for 30 min at 25°C (right panels). Activities of the 26S proteasome in gel-overlay assay were visualized as in Figure 1 with 2 mM ATP. Note that a considerable amount of Hsp90 is associated with the affinity-purified 26S proteasome fraction.

Hsp90 inactivation-induced disassembly of 26S proteasome is reversed by recovery of functional Hsp90. To confirm this attractive conclusion, we analyzed the 26S proteasome 2 h after incubation shown in Figure 3B (right, see arrows) by native PAGE and western blotting using anti-Rpt1. As shown in Figure 3B (right top), changes in activity apparently coincided with reassembly of both the R2C and RC forms of the 26S proteasome.

We next examined the ATP requirement for the Hsp90-dependent reassembly of the 26S proteasome. Depletion of ATP by treatment of cells with metabolic poisons (deoxyglucose and sodium azide) resulted in almost complete dissociation of the 26S proteasome, irrespective of WT and *hsp82-4* cells. When these cells were incubated for 30 min at 37°C in YPD media, reassembly of the 26S proteasome appeared in WT cells following culture in

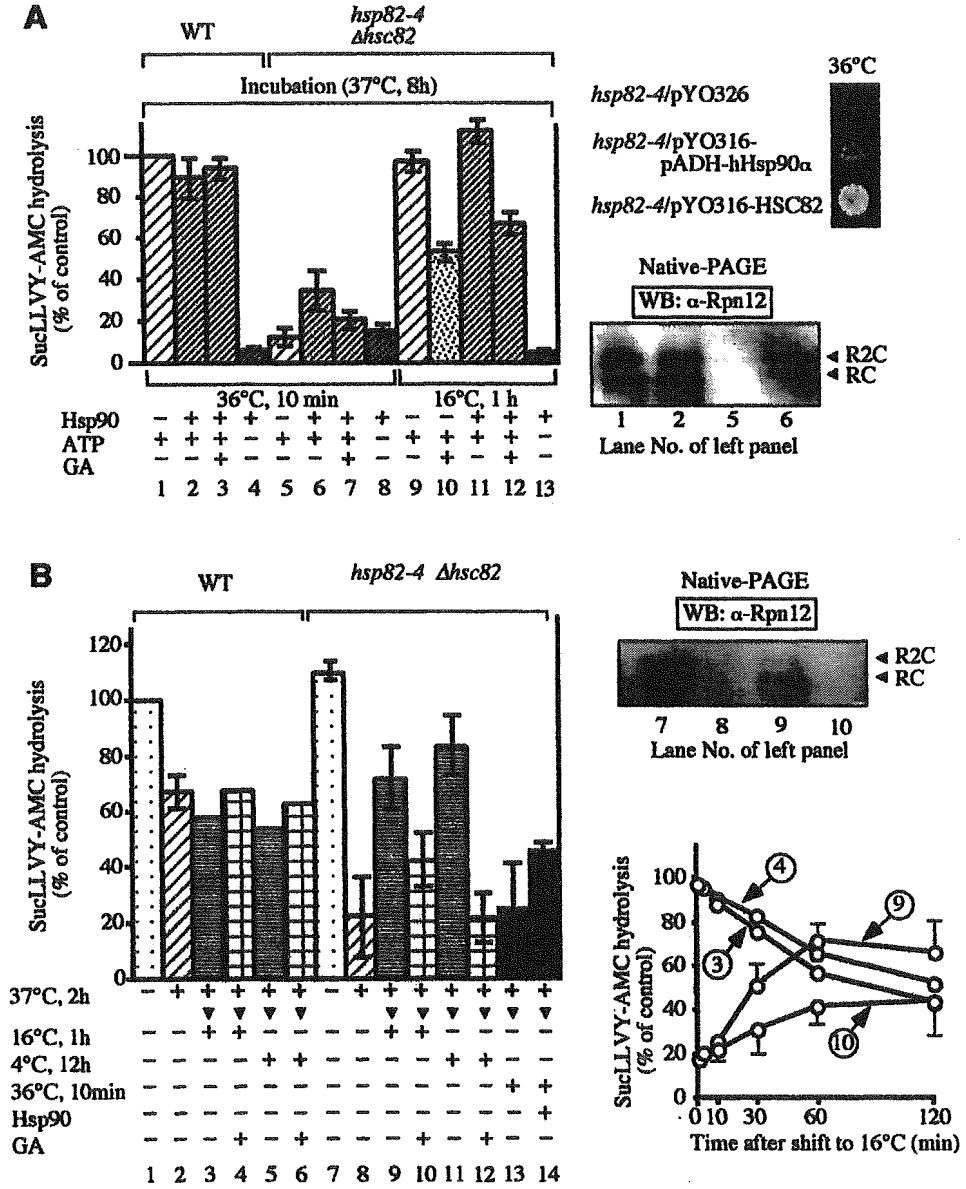

Fig. 4. *In vitro* analyses of the 26S proteasome under conditions with or without Hsp90 inactivation. (A) The Suc-LLVY-AMC degrading activities of the affinity-purified 26S proteasome from WT and *hsp82-4* cells were measured and expressed as percentages of the control (representing the activity of WT cell extracts without incubation). The extracts (10 mg/ml of protein) from both cells grown at 37°C for 8 h were incubated at 36°C for 15 min or at 16°C for 1 h with or without purified Hsp90 (0.1 mg/ml) and in the presence of an ATP-regeneration system (10 mM creatine phosphate, 5 mM $MgCl_2$ and 10 μg/ml of creatine kinase), an ATP-depletion system (10 mM glucose and 1 μg/ml of hexokinase) or GA (18 μM, left). The cell extracts corresponding to lanes 1, 2, 5 and 6 (left) were subjected to native-PAGE, followed by western blotting with anti-Rpn12 (right bottom). Each strain harboring the human-Hsp90α-expressing plasmid (YOK5H/pRS316-hHsp90α), the Hsc82-expressing plasmid (YOK5/pRS316-HSC82) or the vector alone (corresponding empty vector) was spotted on the same plates and incubated at 36°C for 2 days (right top). (B) *In vitro* inactivation and reactivation of the 26S proteasome from *hsp82-4* cells. The affinity-purified 26S proteasome from the same amounts of cell extracts of WT cells (J106) and *hsp82–4Δhsc82* cells (YOK5RH) were maintained at 37°C with an ATP-regenerating system for 2 h and shifted to 16°C for 1 h, 4°C for 12 h or 36°C for 10 min in the presence of an ATP-regenerating system with or without GA (18 μM) or purified Hsp90 (0.1 mg/ml)(left panel). Suc-LLVY-AMC hydrolysis is expressed relative to the activity at time zero of WT cells grown at 25°C. The affinity-purified 26S proteasomes corresponding to lanes 3, 4, 9 and 10 that had been treated at 37°C for 2 h were shifted to 16°C for various times as indicated, and thereafter Suc-LLVY-AMC hydrolysis was assayed as described above (right bottom panel). The affinity-purified 26S proteasomes corresponding to lanes 7–10 were subjected to native PAGE, followed by western blotting with anti-Rpn12 (right top panel). Data in A and B are means ± SEM.

glucose-containing (i.e. ATP-generating) YPD media, but not in *hsp82-4* cells, indicating the indispensable need for ATP in the Hsp90-dependent reassembly of the 26S proteasome (Figure 3C, left). Moreover, GA suppressed the assembly of the 26S proteasome in *hsp82-4* cells, but not WT extracts, at 25°C (Figure 3C, right). Taken together, the above results clearly showed that Hsp90 is required for the *in vivo* reassembly of the 26S proteasome even when this was partial, and, most importantly, the ATPase function of Hsp90 seems to play a pivotal role in this assembly process.

Hsp90-dependent in vitro reassembly of the 26S proteasome

In the next series of experiments, we examined whether Hsp90-dependent dissociation–reassociation of the 26S proteasome occurs in the *in vitro* system. Crude cell extracts were prepared from WT and *hsp82-4* cells grown at 37°C for 8 h, and subsequently incubated at 36°C for 10 min or 16°C for 1 h in the presence of an ATP-regenerating system, ATP-depleting system or GA, and, in some experiments, purified porcine Hsp90 was supplemented. Thereafter, Suc-LLVY-AMC degrading activity was assayed for the 26S proteasome affinity-purified from these cell extracts as shown in Figure 4A (left). The peptidase activity of the purified 26S proteasome decreased to nearly 10% from *hsp82-4* cells upon incubation for 8 h at 37°C compared with 26S proteasome from WT cell extracts, even when ATP was regenerated (see lane 5), but completely disappeared in the absence of ATP irrespective of temperature. Intriguingly, addition of purified Hsp90 caused partial suppression of the reduction in the presence of ATP (lane 6), indicating that Hsp90 is required for the *in vitro* assembly of functional 26S proteasome. Moreover, this Hsp90 effect was ATP dependent, because no obvious protective effect was detected under ATP-depletion conditions (lane 8). Addition of GA partially suppressed this reactivation (lanes 7, 10 and 12). It is noteworthy that *in vitro* reincubation of *hsp82-4* cell extracts for 1 h at 16°C caused almost complete recovery of the peptidase activity irrespective of Hsp90 supplementation (lanes 9 and 11). These findings suggest that Hsp90 promotes ATP-dependent reassembly of the 26S proteasome that had been dissociated by ts^--dependent Hsp90 inactivation.

We also confirmed that the activity change was proportional to the amounts of the purified 26S proteasome detected by western blotting with anti-Rpn12 (Figure 4A, bottom right). No appreciable amounts of the 26S proteasome were adsorbed by the Ni^+-resin column due to their disassembly in extracts of *hsp82-4* cells incubated *in vitro* at a restricted temperature. However, incubation of the same extracts supplemented with purified Hsp90 caused association of considerable amounts of the 26S proteasome with the affinity column, although the level of the recovered proteasome was somewhat low compared with similarly treated extracts of WT cells. These results indicate that Hsp90 is required for the *in vitro* reassembly of the 26S proteasome. Consistent with this notion, *in vivo* forced expression of Hsp90 rescued the growth defect of *hsp82-4* cells under non-permissive conditions, although yeast Hsc82 was effective compared with human Hsp90α (Figure 4A, right top).

To assess the above conclusion further, the 26S proteasome was inactivated and reactivated *in vitro* using the Ni^+-resin 26S proteasome purified from WT and *hsp82-4* cells grown at 25°C. Note that a considerable amount of Hsp90 is associated with the affinity-purified 26S proteasome fraction (see Figure 3A). Under incubation for 2 h at non-permissive temperature of 37°C, the purified 26S proteasome from *hsp82-4* cells showed rapid reduction of the peptidase activity, unlike WT enzymes, even after addition of an ATP-regeneration system (Figure 4B, left panel, lanes 2 and 8). This reduced activity of the 26S proteasome after 2 h of incubation at 37°C was markedly increased after incubation at 16°C for 1 h (lane 9) or at 4°C for 12 h (lane 11) in the presence of an ATP-regeneration system. However, no appreciable restoration of the peptidase activity was observed when an ATP-depletion system was added during incubation at 16°C or 4°C (data not shown), indicating again that metabolic energy is necessary for reactivation of the 26S proteasome. Addition of GA partially inhibited this reactivation (lanes 10 and 12), confirming the importance of ATPase function of Hsp90 for the reactivation, and presumably reassembly, of the 26S proteasome *in vitro*. In addition, such restoration was observed under *in vitro* incubation up to 60 min, which was clearly abrogated by addition of GA, although the activities of WT enzymes were gradually decreased, irrespective of GA (right bottom panel). In accordance with these results, when the 26S proteasome from *hsp82-4* cells that had been treated at 37°C for 2 h was incubated for 10 min at 36°C with purified Hsp90, the peptidase activity was partly recovered (Figure 4B, left panel, lanes 13 and 14). We also confirmed that the change in activity was proportional to the amount of the 26S proteasome detected by western blotting with anti-Rpn12 (Figure 4B, right top panel).

Genetic interactions between HSC82/HSP82 and genes encoding subunits of regulatory particle

To investigate the above findings *in vivo*, we examined genetic interactions using various proteasome mutants (Figure 5A). The *hsp82–4Δhsc82* double mutant showed severe growth defects when combined with mutants of *rpn1-1*, *Δrpn2* and *rpn3-1*. Although each parental strain showed no or only a weak growth defect at 30°C, the resultant triple mutants showed no growth at 30°C. When the combination of *rpn12-1* was examined, the effect was more severe because growth arrest occurred even when the cells were cultured at 25°C. Combination with *Δrpn10* was most surprising; the resultant triple mutant did not grow at all even at 25°C, although *Δrpn10* single mutation showed no growth defect even at 37°C (Figure 5B). On the other hand, overexpression of *HSC82* suppressed the ts^- growth defects of several mutants of the RP subunits of the 26S proteasome, such as *rpn1-1* cells, *Δrpn2* cells and *rpn3-1* cells (Figure 5C, top). Surprisingly, overexpression of Hsc82 inhibited the growth of *Δrpn10* cells and *rpn12-1* cells when they were cultured at 36°C and 25°C, respectively. At both temperatures, cells lacking the ectopically expressed Hsc82 showed no appreciable growth defect (Figure 5C, bottom). Thus genetic interactions between *HSC82/HSP82* and the genes encoding the RP subunits are strong, implying substantial interactions of the Hsp90 and the 26S proteasome.

In addition, even under permissive temperature of 25°C, GA caused severe growth defects in Δ*rpn10* and *rpn12-1* cells (Figure 5D, bottom), though its influence was less in *rpn1-1* and Δ*rpn2* cells (top). On the other hand, *Rpn3-1* cells showed obvious growth defect upon addition of GA at 30°C, but not at 25°C (Figure 5D, bottom). These findings support the genetic interactions between *HSC82/HSP82* and several proteasome genes.

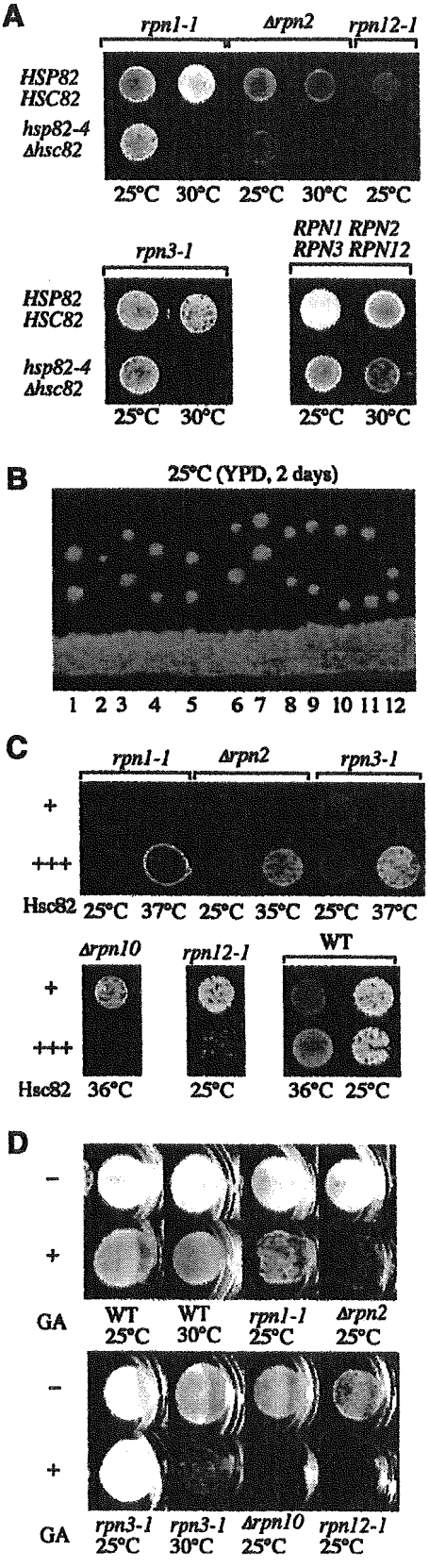

Effects of Hsc82 overexpression on 26S proteasome assembly in various proteasome mutants

Finally, we examined why overexpression of Hsp90 had opposing effects on cell proliferation, which was dependent on the type of mutation against the RP subunits of the 26S proteasome. Since our results showed that Hsp90 influenced the assembly of the 26S proteasome, we examined the role of Hsp90 on the 26S proteasome assembly. Since *HSC82* served as a multicopy suppressor of the temperature-sensitive growth of *rpn1-1* cells, Δ*rpn2* cells and *rpn3-1* cells (Figure 5C, top), we examined the molecular species of the proteasome in these cells using native PAGE followed by western blotting using anti-20S proteasome. Overexpression of Hsc82 suppressed the disassembly of the 26S proteasome in *rpn1-1* cells, Δ*rpn2* cells and *rpn3-1*cells under non-permissive temperatures of 37°C (*rpn1-1* cells and *rpn3-1* cells) and 34°C (Δ*rpn2* cells) (Figure 6A, middle and bottom panels), while absence of such overexpression markedly affected the disassembly of the 26S proteasome. In contrast, the inhibitory effects of overexpression of Hsc82 on Δ*rpn10* cells and *rpn12-1*cells (Figure 5C) appeared to be the results of disassembly of the 26S proteasome in these cells (Figure 6A, bottom). Note the appearance of several bands in these experiments, which were different from the main three bands observed initially which represented the 20S proteasome and the symmetric and asymmetric forms of the 26S proteasome. These extra bands represented incompletely assembled forms of the 26S proteasome, perhaps out by several components, because reactive bands by western blotting with anti-Rpt1 and anti-Rpn12 differed from each other and those with anti-20S proteasome (Figure 6A, middle). Furthermore, we confirmed peptidase activities of these extra bands by the in-gel peptidase assay (Figure 6B). Since the effects of overexpression of Hsc82 in various proteasome mutants correlate with the presence of the functional 26S proteasome, the above results also suggest that Hsp90 plays an important role in the regulation of assembly and disassembly of the 26S proteasome *in vivo*.

Fig. 5. Genetic interactions between HSC82/*HSP82* and various *RPN* genes. (**A**) Growth defects of triple mutants with *hsp82–4Δhsc82* together with *rpn1-1* (J821), Δ*rpn2* (J822), *rpn3-1* (J823) or *rpn12-1* (J8212). Each strain was spotted on YPD and incubated at the indicated temperatures for 2 days. (**B**) Synthetic lethality in Δ*rpn10* and *hsp82–4Δhsc82* mutations. JD8210 cells were sporulated and dissected. No germination of a Ura$^+$ His$^+$ Leu$^+$ colony corresponding to triple mutants was noted. Germination of small colonies was noted, though rarely (e.g. lanes 3 and 8). (**C**) Effects of overexpression of Hsc82. Each strain harboring HSC82 (+++) overexpressing plasmid (YPH500/pYO326-HSC82, JR1/pYO323-HSC82, JR2/pYO323-HSC82, JR3/pYO325-HSC82, JR10/pYO326-HSC82, JR12/pYO326-HSC82) and the vector alone (corresponding empty vector) (+) was spotted on SD plates containing appropriate amino acids and incubated at the indicated temperatures for 2 days. Note that the expressed levels of Hsc82 were not affected by these proteasomal mutations (data not shown). (**D**) Sensitivity to GA in various *rpn* mutants. Each strain used in A was spotted with or without GA (18 μM) and incubated for 2 days at indicated temperatures.

Discussion

The 26S proteasome is an unusually large complex, consisting of two subcomplexes, CP and RP. A major challenge to our understanding of the quaternary structure is how the large complex, composed of many subunits of various sizes, is accurately assembled in the cells. Recent studies of 20S proteasome assembly have shown that a key molecule termed 'Ump1' functions as a core factor to gather multiple proteasomal β-subunits (Ramos *et al.*, 1998). At present, however, little is known about the mechanism(s) involved in the assembly of the 26S proteasome, especially the RP complex.

In the present study, we showed that inactivation of Hsp90, using yeast mutants, caused almost complete disassembly of the 26S proteasome, indicating that Hsp90 plays a role in keeping the structural integrity of this large complex (Figure 2). Inactivation of Hsp90 resulted in dissociation of the 26S proteasome into the core 20S particle, which settled into a latent state, as evidenced by the marked activation upon the addition of SDS (Figure 2A). In contrast, Rpn9 and Rpn12 subunits migrated to different positions in native PAGE (Figure 2E), indicating loss of integrity of the lid complex. However, it is not known whether these lid subunits dissociated into their monomeric forms. It is also not known how Hsp90 influences the organization of the base complex, but it is clear at least that the functional loss of Hsp90 triggers disruption of the RP complex. These findings indicate that the RP complex is structurally fragile, requiring continuous supply of a functional Hsp90 to assemble and maintain these complexes, unlike the 20S proteasome, which is apparently stable without functional Hsp90. Thus the assemblies of the CP/20S proteasome and RP complexes are mechanistically different.

The genetic evidence provided in the present study also strongly suggests *in vivo* linkage between Hsp90 and the 26S proteasome. In fact, we demonstrated that overexpression of Hsc82 suppressed ts⁻ growth defects of *rpn1-1* cells, Δ*rpn2* cells and *rpn3-1* cells (Figure 5C) and prevented dissociation of the 26S proteasome, which occurred under conditions otherwise non-permissive for these mutants (Figure 6). Consistent with this genetic interaction, *hsp82–4Δhsc82* showed weak synthetic lethality with those proteasomal mutations (Figure 5A). Furthermore, strong synthetic lethality was observed between *hsp82–4Δhsc82* and Δ*rpn10* or *rpn12-1*. Interestingly, even though the Δ*rpn10* mutation itself showed no growth defect at all, it exhibited the most severe growth defect when combined with *hsp82–4Δhsc82* mutant (Figure 5B and D). However, overexpression of Hsc82 in Δ*rpn10* cells and *rpn12-1* cells enhanced their growth defects and was associated with decreased 26S proteasome levels in these two strains (Figure 6). One possible explanation for these antagonizing effects is that the tight interaction between Hsp90 and some subunits of regulatory particle might hinder them from proper formation of the 26S proteasome, leading to inhibition of cellular proliferation.

We obtained evidence that a larger amount of Hsp90 is associated with the 26S proteasome from *hsp82-4* cells grown at permissive temperature, compared with the WT proteasome, irrespective of the lower content of Hsp90 in mutant cell extracts (Figure 3A, left), suggesting that the larger amount of mutant Hsp90 might be required to maintain the 26S proteasome because of its functional impairment. We also found that considerable amounts of Hsp90 are associated with the 26S proteasome through the RP complex, and this association is so tight that it occurs even under low Hsp90 conditions in which many other client proteins were dissociated from Hsp90 (Figure 3A, right). In addition, *hsp82-4* cells showed a faster decay of

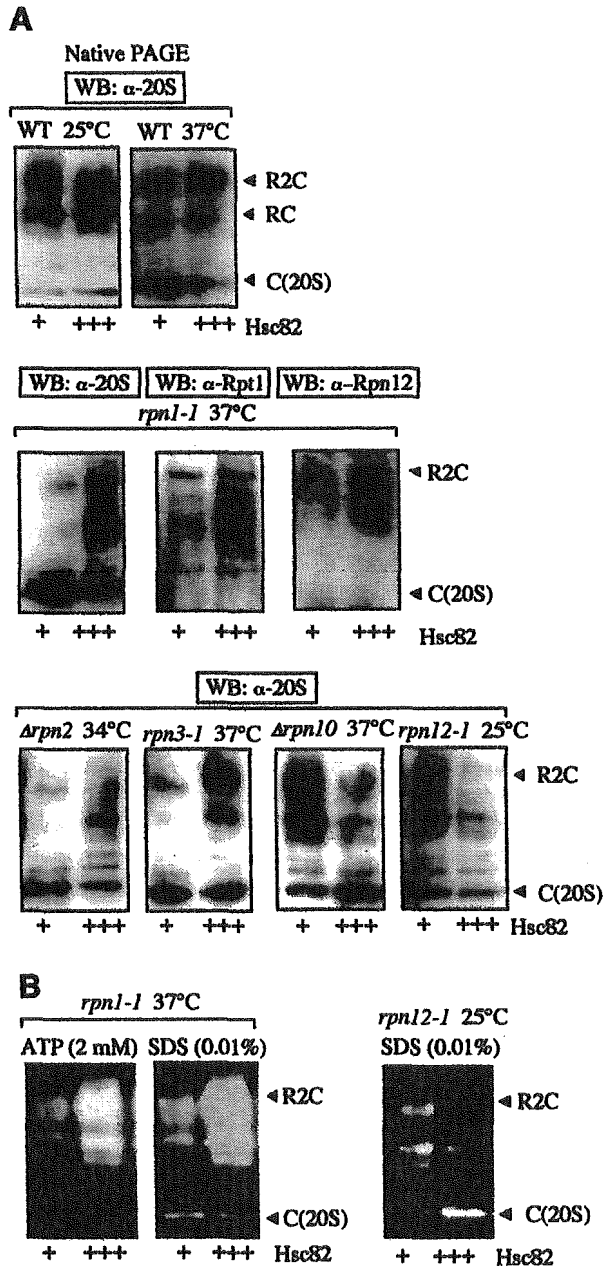

Fig. 6. Effects of overexpression of Hsc82 on the 26S proteasome assembly in various *rpn* mutants. (A) WT cells and various proteasome mutant cells harboring control plasmid (+), multicopy plasmid carrying *HSC82* (+++), as in Figure 5C, grown at 25°C were shifted to the indicated temperatures and incubated for an additional 8 h. Samples of cell lysates (5 μg) were loaded onto native PAGE and analyzed by western blotting with anti-20S proteasome, anti-Rpt1 or anti-Rpn12. (B) Corresponding cell extracts as in (A) were analyzed by gel-overlay assay as in Figure 1 with 2 mM ATP or 0.01% SDS.

Table I. Yeast strains used in this study

Strain	Source	Genotype
YPH500	*MATα ura3 lys2 ade2 trp1 his3 leu2*	Sikorski and Hieter, 1989
YOK5	*MATa ura3 lys2 ade2 trp1 his3 leu2 Δhsc82::URA3 hsp82-4::LEU2*	Kimura *et al.*, 1994
YOK5H	*MATa ura3 lys2 ade2 trp1 his3 leu2 Δhsc82::HIS3 hsp82-4::LEU2*	Our laboratory stock
YOK5RH	*MATa ura3 lys2 ade2 trp1 his3 leu2 Δhsc82::HIS3 hsp82-4::LEU2 6×His-RPT1::URA3*	Present study
5CG2	*MATa ura3 lys2 ade2 trp1 his3 leu2 Δhsc82::URA3 hsp82-4::GAL1-HSP82::LEU2*	Kimura *et al.*, 1994
J106	*MATα 6×His-RPT1::URA3 ura3 lys2 ade2 trp1 his3 leu2*	Takeuchi *et al.*, 1999
YK109	*MATa ura3 lys2 ade2 trp1 his3 leu2 rpn12-1*	Kominami *et al.*, 1997
JR1	*MATa ura3 lys2 ade2 trp1 his3 leu2 rpn1-1*	Present study
J821	*MATa ura3 lys2 ade2 trp1 his3 leu2 Δhsc82::HIS3 hsp82-4::LEU2 rpn1-1*	Present study
JR2	*MATa ura3 lys2 ade2 trp1 his3 leu2 Δrpn2::URA3*	Present study
J822	*MATa ura3 lys2 ade2 trp1 his3 leu2 Δhsc82::HIS3 hsp82-4::LEU2 Δrpn2::URA3*	Present study
JR3	*MATa ura3 lys2 ade2 trp1 his3 leu2 rpn3-1::HIS3*	Present study
J823	*MATa ura3 lys2 ade2 trp1 his3 leu2 Δhsc82::URA3 hsp82-4::LEU2 rpn3-1::HIS3*	Present study
JR10	*MATa ura3 lys2 ade2 trp1 his3 leu2 Δrpn10::HIS3*	Present study
JR12	*MATa ura3 lys2 ade2 trp1 his3 leu2 rpn12-1*	Present study
J8212	*MATa ura3 lys2 ade2 trp1 his3 leu2 Δhsc82::HIS3 hsp82-4::LEU2 rpn12-1*	Present study
J38	*MATα leu2 his3 ura3 trp1 Δrpn10::HIS3*	Takeuchi *et al.*, 1999
JD8210	*MATa/α ura3/ura3 lys2/lys2 ade2/ade2 trp1/trp1 his3/his3 leu2/leu2 Δhsc82::URA3/Δhsc82::URA3 hsp82-4::LEU2/hsp82-4::LEU2 RPN10/Δrpn10::HIS3*	Present study
rpn1::URA3	*MATα ura3 lys2 ade2 trp1 his3 leu2 rpn1::URA3 (rpn1-1)*	Our laboratory stock
W1646-1C	*MATα leu2 his3 ura3 trp1 ade2 Δrpn2::URA3*	Our laboratory stock
YK137	*MATa leu2 his3 ura3 trp1 rpn3-1::HIS3*	Kominami *et al.*, 1997

the peptidase activities of the 26S proteasome after addition of CHX even under permissive temperature compared with WT cells (Figure 3B). Taken together, these results suggest that the 26S proteasome is the most important substrate for Hsp90, and Hsp90 is continually required for maintenance of the 26S proteasome.

The energy requirement for 26S proteasome assembly has been recognized since the discovery of the 26S proteasome (Armon *et al.*, 1990; Driscoll and Goldberg, 1990; Chu-Ping *et al.*, 1994), but the molecular mechanisms of ATP consumption have remained elusive. In the present study, we have provided evidence that ATPase of Hsp90 plays an active role in supplying energy required for the 26S proteasome assembly. Thus, we have shown that the dissociated constituents of the 26S proteasome from *hsp82-4* cells under non-permissive conditions, reassembled *in vivo* and *in vitro* by reactivation of ts$^-$ Hsp82 or addition of purified Hsp90 (Figures 3 and 4). Although the reason for not being able to get the full restoration by purified Hsp90 *in vitro* is not clear at present, it is plausible that Hsp90 acts in concert with various cochaperones, such as p23 (Young *et al.*, 2001), to exert its full activity, some of which might be lost in the purification of Hsp90 by the present technique. More importantly, we demonstrated that ATP is required for Hsp90-dependent reassembly and that inhibition of Hsp90-ATPase function by GA also blocked in part this restoration of the 26S proteasome. Thus we propose that the energy required for the assembly of the 26S proteasome is at least utilized by Hsp90.

An important question is whether the dissociation–association cycle of the 26S proteasome has any physiological significance. An intriguing scenario is that a dissociation–association cycle might be envisaged for the 26S proteasome or it might be regulated to respond to changes in certain environmental circumstances in cells. For example, marked increases have been found in the amounts of the 26S proteasome during the stationary phase compared with those in logarithmically growing yeast cells (Fujimuro *et al.*, 1998). In this regard, it is interesting to note that yeast Hsp90 also increases during the stationary phase (Iida and Yahara, 1984), implying that Hsp90 may contribute to these dynamic alterations, repeating assembly and disassembly in logarithmic/stationary phase shift. In addition, the involvement of an Hsp90 chaperone in the assembly of the 26S proteasome indicates that changes in the physiological state of Hsp90 may alter the amounts of the 26S proteasome. In fact, we initially found that the amounts of the 26S proteasome decreased upon exposure to the thermal insult of 50°C but showed full recovery within 6–8 h after the temperature was reversed to 25°C (Figure 1). In this regard, previous studies reported that the cellular ATP level remained largely unchanged under such severe heat shock conditions (Jamsa *et al.*, 1995), indicating that disassembly of the 26S proteasome is not due to reduced availability of ATP. However, such temporary reductions in the 26S proteasome are conceivable because while Hsp90 is required for the 26S proteasome assembly, it is also responsible for refolding stress-damaged proteins and thereby might be sequestered to those damaged proteins after severe thermal insults. Thus it is conceivable to view the disassembly of the 26S proteasome as a stress response regulated by Hsp90. In other words, our results highlight the importance of Hsp90 in the disassembly–reassembly cycle of the 26S proteasome, although further studies are necessary to determine its precise molecular action.

Materials and methods

Microbiological techniques

Experimental methods for yeast were performed as described (Guthrie and Fink, 1991). Yeast cells were cultured in YPD on logarithmically growing phase, unless otherwise indicated.

Plasmids

Plasmids pYO323-HSC82 and pYO325-HSC82 carry the 4.2 kbp *SpeI*–*SpeI* fragments of *HSC82* in the *XbaI* site of pYO323 and pYO325 (Ohya *et al.*, 1991), respectively. Plasmids pYO326-HSC82 (Imai and Yahara, 2000) and pRS316-pADH-hHsp90α were our laboratory stock.

Antibodies and reagents

Rabbit polyclonal anti-Rpn9 and anti-Rpn12 antibodies were a kind gift from Dr A.Toh-e (Tokyo University). Rabbit polyclonal anti-Rpt1 (Takeuchi *et al.*, 1999), anti-20S proteasome (Tanaka *et al.*, 1988) and anti-Hsp82 (Imai and Yahara, 2000) antibodies were used. Purified porcine Hsp90 was our laboratory stock. Suc-LLVY-AMC was obtained from Peptide Institute Inc. CHX, deoxyglucose and azide were purchased from Sigma Chemical Co. (St Louis, MO). GA was obtained from Gibco BRL (Gaithersburg, MD). Protein concentration was determined using BCA protein assay reagent (Pierce Chemical Co.) with bovine serum albumin (Sigma) as the standard.

Strains

The yeast strains used are listed in Table I. Strains referred to in this study were constructed by conventional genetic methods.

Electrophoresis

We used 10–20% and 7.5–15% (Figure 2B only) gradient gel for SDS–PAGE and 2–15% polyacrylamide gradient gel (Daiichi Pure Chemical Co.) for native PAGE.

Western blotting

The crude cell extracts were subjected to SDS–PAGE or native PAGE, transferred onto a PVDF membrane. Then the blot was developed with the indicated primary antibodies, horseradish peroxidase conjugated secondary antibodies and the chemiluminescent substrate.

Peptidase activity

Peptidase activity was assayed using Suc-LLVY-AMC as a substrate. Suc-LLVY-AMC (0.1 mM) was incubated with an enzyme source for 10 min at 37°C as described previously (Tanaka *et al.*, 1988). The activities are expressed as averages of three independent experiments or as mean ± SEM. The overlay assay of peptidase activities of the proteasome after native PAGE was described previously (Glickman *et al.*, 1998). Peptidase activity was visualized by irradiating the gel with 380 nm UV light.

Preparation of crude extracts

Yeast cells were harvested and washed once with ice-cold lysis buffer (100 mM Tris–HCl pH 7.6, 2 mM ATP, 0.5 mM EDTA, 2 mM $MgCl_2$ and 2% glycerol), and then disrupted with glass beads in 200 µl of lysis buffer. After removal of unbroken cells and glass beads by brief centrifugation at 100 *g*, the extracts were clarified by centrifugation twice at 20 000*g* and 4°C for 10 min. The final supernatant was used as the crude extract.

Affinity-purification of 26S proteasome

Purification of 26S proteasome by Ni-nitrilotriacetic acid (NTA) affinity chromatography was performed. Briefly, the yeast extracts were clarified by centrifugation at 100 000 *g* at 4°C for 30 min. The supernatant was subjected to ultracentrifugation at 235 000 *g* and 4°C for 5 h to precipitate the proteasome. The resulting precipitates were gently dissolved in 10 ml of buffer A (20 mM Tris–HCl pH 7.8, 1 mM ATP, 0.1 mM EDTA, 2 mM $MgCl_2$, 100 mM NaCl and 10% glycerol) with an ATP regeneration system. After removal of insoluble materials by centrifugation at 9100 *g* and 4°C for 10 min, the resulting supernatant was loaded onto a Ni^+-NTA–agarose column (Qiagen, Hilden, Germany). After washing the column with buffer A containing 50 mM imidazole, the His-tagged column associated with the proteasome was eluted with elution buffer (buffer A with 200 mM imidazole). In successive experiments, the 26S proteasome was purified from the same volume of cell extracts containing the same amount of protein.

References

Armon,T., Ganoth,D. and Hershko,A. (1990) Assembly of the 26S complex that degrades proteins ligated to ubiquitin is accompanied by the formation of ATPase activity. *J. Biol. Chem.*, **265**, 20723–20726.

Baumeister,W., Walz,J., Zuhl,F. and Seemuller,E. (1998) The proteasome: paradigm of a self-compartmentalizing protease. *Cell*, **92**, 367–380.

Chu-Ping, M., Vu,J. H, Proske,R.J., Slaughter,C.A. and DeMartino,G.N. (1994) Identification, purification and characterization of a high molecular weight, ATP-dependent activator (PA700) of the 20S proteasome. *J. Biol. Chem.*, **269**, 3539–3547.

Driscoll,J. and Goldberg,A.L. (1990) The proteasome (multicatalytic protease) is a component of the 1500-kDa proteolytic complex which degrades ubiquitin-conjugated proteins. *J. Biol. Chem.*, **265**, 4789–4792.

Frydman,J. (2001) Folding of newly translated proteins *in vivo*: the role of molecular chaperones. *Annu. Rev. Biochem.*, **70**, 603–647.

Fujimuro,M., Takada,H., Saeki,Y., Toh-e,A., Tanaka,K. and Yokosawa,H. (1998) Growth-dependent regulation of the 26S proteasome assembly in the budding yeast *Saccharomyces cerevisiae*. *Biochem. Biophys. Res. Commun.*, **251**, 818–823.

Glickman,M.H., Rubin,D.M., Coux,O., Wefes,I., Pfeifer,G., Cjeka,Z., Baumeister,W., Fried,V.A. and Finley,D. (1998) A subcomplex of the proteasome regulatory particle required for ubiquitin-conjugate degradation and related to the COP9 signalosome and eIF3. *Cell*, **94**, 615–623.

Guthrie,C. and Fink,G.R. (eds) (1991) Guide to yeast genetics and molecular biology. Academic Press, San Diego, CA.

Iida,H. and Yahara,I. (1984) Durable synthesis of high molecular weight heat shock proteins in G_0 cells of the yeast and other eucaryotes. *J. Cell Biol.*, **99**, 199–207.

Imai,J. and Yahara,I. (2000) Role of HSP90 in salt stress tolerance via stabilization and regulation of calcineurin. *Mol. Cell. Biol.*, **20**, 9262–9270.

Jamsa,E., Vakula,N., Arffman,A., Kilpelainen,I. and Makarow,M. (1995) *In vivo* reactivation of heat-denatured protein in the endoplasmic reticulum of yeast. *EMBO J.*, **14**, 6028–6033.

Kimura,Y., Matsumoto,S. and Yahara,I. (1994) Temperature-sensitive mutants of hsp82 of the budding yeast *Saccharomyces cerevisiae*. *Mol. Gen. Genet.*, **242**, 517–527

Kominami,K. *et al.* (1997) Yeast counterparts of subunits S5a and p58 (S3) of the human 26S proteasome are encoded by two multicopy suppressors of nin1-1. *Mol. Biol. Cell*, **8**, 171–187.

Ohya,Y., Umemoto,N., Tanida,I., Ohta,A., Iida,H. and Anraku,Y. (1991) Calcium-sensitive cls mutants of *Saccharomyces cerevisiae* showing a Pet^- phenotype are ascribable to defects of vacuolar membrane H(+)-ATPase activity. *J. Biol. Chem.*, **266**, 13971–13977.

Panaretou B., Prodromou C., Roe S.M., O'Brien R., Ladbury J.E., Piper P.W. and Pearl L.H. (1998) ATP binding and hydrolysis are essential to the function of the Hsp90 molecular chaperone *in vivo*. *EMBO J.*, **17**, 4829–4836.

Pickart,C.M. (2001) Mechanisms underlying ubiquitination. *Annu. Rev. Biochem.*, **70**, 503–533.

Ramos,P. C, Hockendorff,J., Johnson,E.S., Varshavsky,A. and Dohmen,R.J. (1998) Ump1p is required for proper maturation of the 20S proteasome and becomes its substrate upon completion of the assembly. *Cell*, **92**, 489–499.

Richter,K. and Buchner,J. (2001) Hsp90: chaperoning signal transduction. *J. Cell. Physiol.*, **188**, 281–290.

Sherman,M.Y. and Goldberg,A.L. (2001) Cellular defences against unfolded proteins: a cell biologist thinks about neurodegenerative diseases. *Neuron*, **29**, 15–32.

Sikorski,R.S. and Hieter,P. (1989) A system of shuttle vectors and yeast host strain designed for efficient manipulation of DNA in *Saccharomyces cerevisiae*. *Genetics*, **122**, 19–27.

Takeuchi,J., Fujimuro,M., Yokosawa,H., Tanaka,K. and Toh-e,A. (1999) Rpn9 is required for efficient assembly of the yeast 26S proteasome. *Mol. Cell. Biol.*, **19**, 6575–6584.

Tanaka,K., Yoshimura,T., Kumatori,A., Ichihara,A., Ikai,A., Nishigai,M., Kameyama,K. and Takagi,T. (1988) Proteasomes (multi-protease complexes) as 20S ring-shaped particles in a variety of eukaryotic cells. *J. Biol. Chem.*, **263**, 16209–16217.

Young,J.C., Moarefi,I. and Hartl,F.U. (2001) Hsp90: a specialized but essential protein-folding tool. *J. Cell Biol.*, **154**, 267–273.

Received January 20, 2003; revised May 20, 2003; accepted May 21, 2003

THE JOURNAL OF BIOLOGICAL CHEMISTRY
Vol. 278, No. 19, Issue of May 9, pp. 16809–16819, 2003
Printed in U.S.A.

Sterol Regulatory Element-binding Proteins Are Negatively Regulated through SUMO-1 Modification Independent of the Ubiquitin/26 S Proteasome Pathway*

Received for publication, December 6, 2002, and in revised form, February 19, 2003
Published, JBC Papers in Press, March 2, 2003, DOI 10.1074/jbc.M212448200

Yuko Hirano, Shigeo Murata‡, Keiji Tanaka‡, Makoto Shimizu, and Ryuichiro Sato§

From the Department of Applied Biological Chemistry, Graduate School of Agricultural and Life Sciences, the University of Tokyo, Tokyo 113-8657 and the ‡Department of Molecular Oncology, Tokyo Metropolitan Institute of Medical Science, Tokyo 113-8613, Japan

Sterol regulatory element-binding proteins (SREBPs) are major transcription factors that activate the genes involved in cholesterol and fatty acid biosynthesis. We here report that the nuclear forms of SREBPs are modified by the small ubiquitin-related modifier (SUMO)-1. Mutational analyses identified two major sumoylation sites (Lys^{123} and Lys^{418}) in SREBP-1a and a single site (Lys^{464}) in SREBP-2. Mutant SREBPs lacking one or two sumoylation sites exhibited increased transactivation capacity on an SREBP-responsive promoter. Overexpression of SUMO-1 reduced whereas its dominant negative form increased mRNA levels of SREBP-responsive genes. Nuclear SREBPs interacted with the SUMO-1-conjugating enzyme Ubc9, and overexpression of a dominant negative form of Ubc9 increased the mRNA levels of SREBP-responsive genes. Pulse-chase experiments revealed that sumoylation did not affect the degradation of SREBPs through the ubiquitin-proteasome pathway. *In vitro* ubiquitylation assay showed no competition between ubiquitin and SUMO-1 for the same lysine. Considered together, our results indicate that SUMO-1 modification suppresses the transactivation capacity of nuclear SREBPs in a manner different from the negative regulatory mechanism mediated by proteolysis.

SREBPs[1] control the transcription of a number of genes encoding enzymes and proteins involved in cholesterol and fatty acid metabolism (1). These transcription factors belong to a large class of transcription factors containing a basic helix-loop-helix leucine zipper (bHLH-Zip) motif. The SREBP family comprises three subtypes: SREBP-1a and SREBP-1c, which are generated by alternative splicing, mainly regulating lipogenic gene expression, and SREBP-2 governing cholesterol metabolism. Unlike other members of the bHLH-Zip transcription factors, the SREBPs are synthesized as membrane-bound precursors on the endoplasmic reticulum (ER) and activated by a two-step proteolytic process (2–4). The precursor proteins contain an N-terminal transcriptional activation domain with a bHLH-Zip motif and a C-terminal regulatory domain separated by two transmembrane regions. The C-terminal regulatory domain associates with SREBP cleavage-activating protein (SCAP), an ER membrane protein with eight membrane-spanning segments, which contains a sterol-sensing domain (5). An SREBP-SCAP complex remains on the ER membrane as long as intracellular cholesterol levels are high, whereas in cells depleted of cholesterol ER-derived membrane vesicles containing this complex moves to the Golgi, where a sequential cleavage of the SREBPs by site 1 and site 2 protease occurs, releasing the active nuclear forms (6). Once the nuclear form of SREBPs is released into the cytoplasm, it is actively transported into the nucleus in an importin β-dependent manner (7). In the nucleus, the SREBPs are modified by polyubiquitin chains and rapidly degraded by the 26 S proteasome (8). In the presence of proteasome inhibitors, ALLN and lactacystin, the stabilized nuclear SREBPs are capable of enhancing their responsive gene expression. Thus, ubiquitylation of the nuclear SREBPs and the subsequent turnover play important roles in regulation of lipid metabolism.

Posttranslational modification of a variety of cellular proteins has been variably linked to protein phosphorylation and acetylation other than ubiquitylation. SUMO-1, a 101-amino acid protein bearing 18% identity with ubiquitin but with a remarkably similar secondary structure, has been recently identified. SUMO-1 differs from ubiquitin in its surface-charge distribution, eliciting its specificity (9), and does not have a consensus sumoylation motif, (I/V/L)KX(E/D), in its molecule, explaining why SUMO-1 does not make multichain forms (10, 11).

Sumoylation requires a multiple-step reaction similar to that of ubiquitin, but the specific enzymes are distinct from those involved in ubiquitylation (12). SUMO-1 is synthesized as a precursor with the C-terminal extension of several amino acids, which needs to be processed to expose the C-terminal Gly^{97} residue that is essential for conjugation to target proteins (13). Then the processed SUMO-1 is recognized as a substrate by SUMO-activating enzyme (E1), which is a heterodimer consisting of SAE1 (also called Uba2) and SAE2 (also called Aos1) subunits (14). Ubc9 is a SUMO-conjugating enzyme (E2), receiving SUMO-1 from the E1 enzyme and transferring it to target proteins (15). Most sumoylated proteins directly interact with Ubc9, which catalyzes the sumoylation of such proteins (16). A recent report showed that Ubc9 recognizes the consensus sequence that surrounds the acceptor lysine residue in sumoylation substrates (17), implying that Ubc9 itself might play to a certain extent a ubiquitin E3-like role in determining the substrate specificity (18). However, recent studies have

* The costs of publication of this article were defrayed in part by the payment of page charges. This article must therefore be hereby marked "*advertisement*" in accordance with 18 U.S.C. Section 1734 solely to indicate this fact.

§ To whom correspondence should be addressed. Fax: 81-3-5841-8026; E-mail: aroysato@mail.ecc.u-tokyo.ac.jp.

[1] The abbreviations used are: SREBP, sterol regulatory element-binding protein; bHLH-Zip, basic helix-loop-helix-leucine zipper; ER, endoplasmic reticulum; SCAP, SREBP cleavage-activating protein; E1, ubiquitin-activating enzyme; E2, ubiquitin carrier protein; E3, ubiquitin-protein isopeptide ligase; HMG, hydroxymethylglutaryl; LDL, low density lipoprotein; Ub, ubiquitin; HA, hemagglutinin; SC, synergy control; GST, glutathione *S*-transferase.

identified ubiquitin ligase (E3)-like ligases for sumoylation that enhance SUMO-1 conjugation to target proteins in yeasts and mammals (19).

In recent years, a growing number of SUMO-1 target proteins including several transcription factors have been reported (20). In contrast to ubiquitylation, which usually marks proteins for rapid degradation, sumoylation is involved in the regulation of protein functions through changes in protein-protein interactions (21, 22), subcellular localization (23), and antagonism to ubiquitylation. Thus, sumoylation serves to enhance the stabilization of target proteins (24) and inhibit DNA repair (25).

The effects of SUMO-1 modification of transcription factors are very diverse, depending on the nature of transcription factors. SUMO-1 modification induces nuclear relocalization of p53 and enhances the DNA-binding ability of heat shock transcription factor 1 and 2, resulting in increased transcriptional activities (26–28). In contrast, sumoylation to p73α does not affect its transcriptional activity but rather its subcellular localization (29), whereas SUMO-1 modification attenuates the transcriptional activities of c-Myb, c-Jun, and androgen receptor (30–32). Thus, SUMO-1 modification might be a common mechanism that regulates specific activities of transcriptional factors.

Here we report a novel posttranslational modification of SREBP-1 and SREBP-2 by the covalent attachment of two molecules and a single molecule of the SUMO-1 protein, respectively. We show that sumoylation does not affect ubiquitylation and the stability but does modulate transcriptional activities of the SREBPs. Our results point to another mechanism through which the SREBPs activities are attenuated in conjunction with degradation by the ubiquitin/26 S proteasome pathway.

EXPERIMENTAL PROCEDURES

Materials—We obtained Redivue Pro-mix L-^{35}S *in vitro* cell labeling mix, glutathione-Sepharose 4B, and Protein A-Sepharose CL-4B from Amersham Biosciences; protease inhibitor mixture and lipoprotein-deficient serum from Sigma; MG-132 (benzyloxycarbonyl-Leu-Leu-Leu-CHO) and *N*-ethylmaleimide from Calbiochem; and iodoacetamide from Fluka (Buchs, Switzerland).

Expression Plasmids—The pSREBP-1a-(1–487) and the pSREBP-2-(1–481) were described previously (33, 34). Expression plasmids pFLSBP-1a-(2–487) and pFLSBP-2-(2–481) were constructed by inserting fragments coding amino acids 2–487 of human SREBP-1a and 2–481 of SREBP-2 into the pCMV-3Flag (Sigma), respectively. To generate expression plasmid pGSTSBP-1a-(2–487) and pGSTSBP-2-(2–481), the fragments were transferred to the pME-GST(6P-3), which was kindly provided by Dr. Tezuka (Institute of Medical Science, University of Tokyo). To generate the expression plasmid pG4-FLSBP-1a-(2–487), the fragment coding amino acids 2–487 of SREBP-1a was ligated into the expression plasmid pM-Flag, which was constructed by inserting a GAL4 DNA-binding domain expression vector, pM (Clontech). The expression plasmid pG4-HisSBP-2-(2–481) was constructed by inserting the fragment for amino acids 2–481 of SREBP-2 into the expression plasmid pM-His, which was engineered to contain the in-frame N-terminal His epitope tag MRGS(H)$_6$. All expression plasmids encoding SREBP mutants were synthesized by a PCR-assisted method using the site-directed mutagenesis kit following the instructions provided by the supplier (Stratagene, La Jolla, CA).

The pEGFP-SUMO-1 was a kind gift from Dr. Minoru Yoshida (RIKEN). The pHA-SUMO-1 was kindly provided by Dr. Chiba (Tokyo Metropolitan Institute of Medical Science). The expression plasmid pHisSUMO was constructed by inserting a fragment encoding human SUMO-1 cloned into the pME-His (8). Expression plasmids pHis-SUMO(GG) and pHisSUMOΔGG were generated by ligating PCR-generated fragments. To construct expression plasmids pHisUbc9 and pGFPUbc9, a fragment of human Ubc9 was amplified by reverse transcriptase-PCR and inserted into the pME-His and the pME-GFP (8). The expression plasmid pHisUbc9(C93S) was generated using the site-directed mutagenesis kit. To generate the pG5Luc reporter plasmid, five copies of Gal4 binding sites in the pG5CAT (Clontech) were transferred to the pGL3-Basic (Promega, Madison, WI).

Antibodies—The anti-SREBP-1 polyclonal antibody RS005 and the anti-SREBP-2 polyclonal antibody RS004 have been described previously (8, 35). The anti-RGS(H)$_4$ monoclonal antibody was purchased from Qiagen (Hilden, Germany); the anti-FLAG monoclonal antibody M2 and anti-GST polyclonal antibody were obtained from Sigma; anti-Ubc9 polyclonal antibody was from Santa Cruz Biotechnology, Inc. (Santa Cruz, CA); anti-multiubiquitin monoclonal antibody was from Medical & Biological Laboratories Co. (Nagoya, Japan); anti-HA monoclonal antibody was from BabCO (Richmond, CA); and anti-GMP-1 (anti-SUMO-1) monoclonal antibody was from Zymed Laboratories (San Francisco, CA).

Cell Lines and Culture Conditions—HeLa, COS-1, HEK293 and M19 cells and site 2 protease null mutant Chinese hamster ovary cells, which were kindly provided by Dr. Chang (Dartmouth College, Hanover, NH), were cultured as described previously (8, 36).

Immunoprecipitation and Immunoblotting—For detection of sumoylated endogenous SREBPs, HeLa cells (20 100-mm dishes) were set up on day 0 in medium A (Dulbecco's modified Eagle's medium; Sigma) supplemented with 10% fetal bovine serum supplemented with 10% fetal bovine serum. On day 1, the cells were transfected with 3 μg of pHA-SUMO-1 using X-tremeGENE Q2 Transfection Reagent (Roche Applied Science). After transfection, the cells were refed with medium A containing 5% lipoprotein-deficient serum, 50 μM pravastatin, and sodium mevalonate. After incubation for 48 h, the cells were harvested with Buffer C* containing 20 mM HEPES/KOH (pH 7.9), 20% glycerol, 1.5 mM $MgCl_2$, 300 mM NaCl, 0.5% Nonidet P-40, and 0.2 mM EDTA supplemented with a mixture of protease inhibitors, 10 μM MG-132, 20 mM *N*-ethylmaleimide, and 10 mM iodoacetamide. After centrifugation at 13,000 × *g* for 10 min at 4 °C, the supernatant was immunoprecipitated by the Seize Classis X Protein A immunoprecipitation kit (Pierce) following the instructions provided by the supplier and resolved on SDS-PAGE and immunoblotted as described previously (8).

COS-1 and M19 cells were set up on day 0. On day 1, the COS-1 cells were transfected using the DEAE-dextran methods and then refed with medium A supplemented with 10% fetal bovine serum. M19 cells were transfected using LipofectAMINE (Invitrogen) and then refed with medium B (a 1:1 mixture of Ham's F-12 medium and Dulbecco's modified Eagle's medium) containing 5% lipoprotein-deficient serum supplemented either with 1 μg/ml 25-hydroxycholesterol plus 10 μg/ml cholesterol (the sterol-loaded condition) or 50 μM pravastatin plus 50 μM sodium mevalonate (the sterol-depleted condition). After incubation for 48 h, the cells were harvested with a radioimmune precipitation buffer containing 50 mM Tris/HCl (pH 7.8), 150 mM NaCl, 5 mM EDTA, 15 mM $MgCl_2$, 1% Nonidet P-40, 0.75% sodium deoxycholate, 1 mM dithiothreitol for binding assays or Buffer C* for sumoylation assays supplemented with a mixture of protease inhibitors, 10 μM MG-132, 20 mM *N*-ethylmaleimide, and 10 mM iodoacetamide. After centrifugation at 13,000 × *g* for 10 min at 4 °C, the supernatant was incubated with 50 μl of a 50% slurry of glutathione-Sepharose 4B or immunoprecipitated with the indicated antibodies and 50 μl of a 50% slurry of Protein A-Sepharose CL-4B. All resins were resolved on SDS-PAGE and immunoblotted as described previously (8).

Northern Blotting—HeLa cells (5 × 10^5 cells/60-mm dish) transfected with various expression plasmids were cultured under the sterol-depleted condition for 48 h and then harvested. Northern blot analysis was performed as described previously (34, 37). Membranes transferring total RNA were hybridized with radioactive cDNA probes, human hydroxymethylglutaryl (HMG)-CoA synthase, LDL receptor, and glyceraldehyde-3-phosphate dehydrogenase.

Reporter Assays—Reporter Assays were performed as described previously (36). HEK293 cells were transfected with 0.2 μg of the pLDLR (38) or the pG5Luc, 0.01 μg of the pRL-CMV, an expression plasmid encoding *Renilla* luciferase (Promega), and the indicated amounts of various expression plasmids. After incubation for 48 h, the Dual-Luciferase™ Reporter System (Promega) was used to determine luciferase activities.

Pulse-Chase Experiments—On day 0, monolayers of COS-1 cells were set up and transfected on day 1 with wild-type or mutant SREBPs. One day after transfection, the cells were trypsinized and reseeded to normalize the transfection efficiency. On day 3, the cells were preincubated for 1 h with methionine/cysteine-free medium A (Invitrogen) supplemented with 10% fetal bovine serum and then pulsed with 200 μCi of L-^{35}S cell labeling mix for 1 h. After the pulse period, the cells were incubated for 1 h and then washed with phosphate-buffered saline and refed with a prewarmed complete medium. After each chase period, the cells were harvested and lysed with a cold lysis buffer containing 10 mM Tris/HCl (pH 7.4), 0.1% Triton X-100, 0.1% SDS, and 2 mM EDTA. The immunoprecipitates with anti-FLAG antibodies were visualized by au-

A

potential sumoylation sites in nuclear SREBPs

Consensus sequence		(I/V/L)K(Q/T)E
SREBP-1a	120-128	PGI**K**[123]EESVP
	378-386	QKL**K**[381]QENLS
	415-423	EGV**K**[418]TEVED
	467-475	SKA**K**[470]PEQRP
SREBP-2	417-425	VDL**K**[420]IEDFN
	461-469	AKV**K**[464]DEPDS

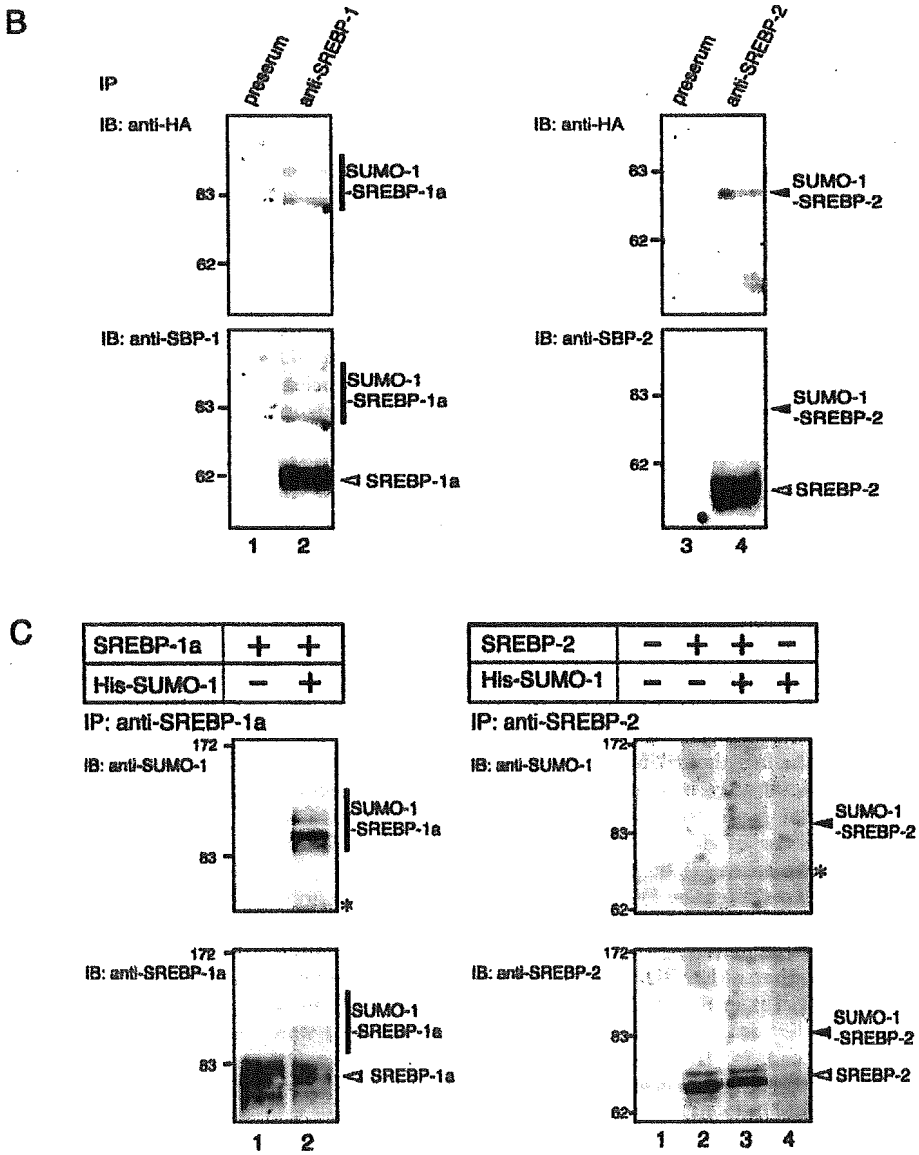

FIG. 1. **Nuclear forms of SREBPs are covalently modified by SUMO-1.** *A*, potential SUMO-1 modification sites in nuclear SREBPs. The amino acid sequences of the sumoylation consensus motif and closest matches in human nuclear SREBP-1a and SREBP-2 are listed. Numbering of the nuclear SREBPs amino acid sequences is shown on the *left*. Potential sumoylation sites are highlighted by *boldface characters*. *B*, HeLa cells were transfected with an expression plasmid encoding HA-SUMO-1. After 48 h of culture, the cell extracts were subjected to immunoprecipitation (*IP*) with either preimmune serum, anti-SREBP-1 (*left*), or anti-SREBP-2 (*right*) antibodies and immunoblotting (*IB*) with anti-HA (*top*) and SREBP-1/2 (*bottom*) antibodies. The mobilities of the SUMO-1-modified and -unmodified SREBPs are indicated on the *right*. The positions of molecular mass standards are marked on the *left*.

toradiography. Exposed filters were quantitatively analyzed on Fluor-Image Analyzer with Image Gauge (Fuji Film).

In Vitro Ubiquitylation Assay—The ubiquitylation assay was previously described (39). Substrate GST-SREBPs were prepared from COS-1 cells transfected with pGSTSBPs. The cells were treated with 20 μM MG-132 for the last 12 h of the culture and then lysed. The GST-SREBPs immobilized on the glutathione-Sepharose 4B were incubated with 40 ng of E1, 0.4 μg of E2, and 8.0 μg of GST-Ub in 40 μl of the ubiquitylation buffer containing 50 mM Tris/HCl (pH 7.5), 2 mM $MgCl_2$, 1 mM dithiothreitol, and 4 mM ATP for 3 h at 37 °C. The reactions were terminated by the addition of the SDS sample buffer.

RESULTS

Posttranslational Modification of Endogenous SREBPs by Covalent Attachment of SUMO-1—Analysis of the amino acid sequences of the nuclear forms of human SREBPs revealed that SREBP-1a contains four matches to the consensus sumoylation sequence centered around Lys^{123}, Lys^{381}, Lys^{418}, and Lys^{470}, and that SREBP-2 contains two matches, centered around Lys^{420} and Lys^{464} (Fig. 1*A*). To examine whether the endogenous SREBPs are modified by SUMO-1, HeLa cells were

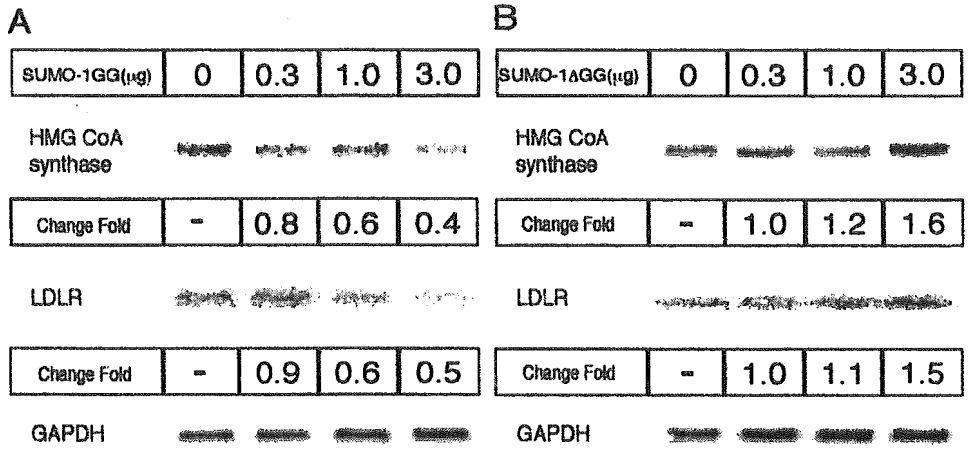

FIG. 2. **A dominant-negative form of SUMO-1 induces the expression of SREBP-responsive genes.** HeLa cells in a 60-mm dish were transfected with the indicated amounts of expression plasmids, either His-SUMO-1(GG) (*A*) or His-SUMO-1ΔGG (*B*). After transfection, the cells were cultured under sterol-depleted conditions for 48 h. Total RNA (8 μg/lane) was subjected to electrophoresis and blot hybridization with the indicated ^{32}P-labeled probe as described under "Experimental Procedures." The results were normalized to the signal generated from glyceraldehyde-3-phosphate dehydrogenase (*GAPDH*). The same results were obtained in three separate experiments. *LDLR*, LDL receptor.

transiently transfected with an expression plasmid for HA-SUMO-1 and cultured under sterol-depleted conditions for 48 h to increase in the amount of the nuclear SREBPs. The nuclear extracts treated with isopeptidase inhibitors, *N*-ethylmaleimide and iodoacetamide, were subjected to immunoprecipitation and immunoblot analysis. In the case of SREBP-1a, anti-HA antibodies recognized several slower migrating bands in the immunoprecipitates with anti-SREBP-1 antibodies (Fig. 1*B*, *left top*). Anti-SREBP-1 antibodies also detected weaker bands for SUMO-1-modified forms above the parental form of SREBP-1a (*left bottom*). In the case of SREBP-2, anti-HA antibodies recognized a single band in the immunoprecipitates with anti-SREBP-2 antibodies (*right top*), and anti-SREBP-2 antibodies detected a faint SUMO-1-modified form above the parental form of SREBP-2 (*right bottom*). These results demonstrated that endogenous SREBPs are modified by SUMO-1. Based on the fact that SUMO-1 can be covalently attached to a lysine residue only in a monomeric form (40), our findings suggest that more than two residues of lysine among four potential sites in SREBP-1a and a single residue of lysine between two potential sites in SREBP-2 are modified.

A Dominant Negative Form of SUMO-1 Induces the Expression of SREBP-responsive Genes—To determine whether the transcriptional activities of endogenous SREBPs are regulated by sumoylation, either SUMO-1(GG), a processed mature form of SUMO-1 (13), or SUMO-1ΔGG, a dominant-negative form of SUMO-1 that is unable to attach target proteins (42), was overexpressed in HeLa cells. Northern blot analyses for SREBP-responsive genes shown in Fig. 2 indicate that overexpression of SUMO-1(GG) decreased the amounts of HMG-CoA synthase and LDL receptor mRNA in a dose-dependent manner, suggesting that sumoylated endogenous SREBPs (Fig. 1*B*) down-regulate transcription of their target genes (Fig. 2*A*). In contrast, overexpression of SUMO-1ΔGG increased the amounts of HMG-CoA synthase and LDL receptor mRNA in a dose-dependent manner, indicating that block of sumoylation accelerated transcription of SREBP target genes (Fig. 2*B*). These results indicate that sumoylation of endogenous SREBPs can affect regulation of the SREBP-responsive gene expression.

Two Lys Residues (Lys^{123} and Lys^{418}) in SREBP-1a Are Sumoylated—To determine which Lys residues in SREBP-1a are sumoylated, we cotransfected COS-1 cells with expression plasmids for His-SUMO-1 and either wild-type or mutant versions of GST-SREBP-1a. GST-SREBP-1a bound to glutathione-Sepharose resins were subjected to immunoblotting with anti-SUMO-1 antibodies (Fig. 3, *A* and *B*, *top panels*). Three sumoylated bands were detected in cells transfected with an expression plasmid for wild-type SREBP-1a, whereas a single sumoylated band was detected in cells expressing either SREBP-1a K381R/K418R/K470R or K123R/K381R/K470R (Fig. 3*A*, *top*, *lanes 1*, *2*, and *4*). No bands were observed after the removal of four lysine residues in potential sumoylation sites (*lane 6*). Another immunoblotting analysis with anti-SREBP-1a antibodies confirmed that all sumoylated bands observed in the *top panel* were derived from sumoylated SREBP-1a (*bottom*). It is likely that the most slowly migrating sumoylated band in GST-SREBP-1a (*top*, *lane 1*) represents doubly sumoylated proteins at Lys^{123} and Lys^{418}. Fig. 3*B* also shows that mutation at both Lys^{123} and Lys^{418} completely abolished sumoylation of SREBP-1a (*lane 10*). Mutation of one of two possible sumoylation sites, Lys1^{23} and Lys^{418}, resulted in a single sumoylated band (*lanes 8* and *9*), confirming that these residues are major sumoylation sites. Taken together, these results clearly demonstrate that the molecule of SREBP-1a contains two possible sumoylation sites, Lys^{123} and Lys^{418}.

SREBP-2 Is Sumoylated at Lys^{464}—To determine which Lys residues of two putative sumoylation sites in SREBP-2 are modified, COS-1 cells were transiently transfected with expression plasmids for His-SUMO-1 and either wild-type or mutant versions of SREBP-2. Fig. 4 shows that a slowly migrating SUMO-1-conjugated band (~83 kDa) was detected when either wild-type or K420R SREBP-2 was expressed together with His-SUMO-1. These results clearly indicate that Lys^{464} serves as the sumoylation site in the nuclear form of SREBP-2.

Sumoylation Decreases the Transactivation Activities of SREBPs—To assess the potential consequences of sumoylation of SREBPs, we examined whether sumoylation influences the transcriptional activities of SREBPs. HEK293 cells were co-transfected with a reporter plasmid, pLDLR, containing the promoter region of human low density lipoprotein receptor gene, and expression plasmids encoding either wild-type or

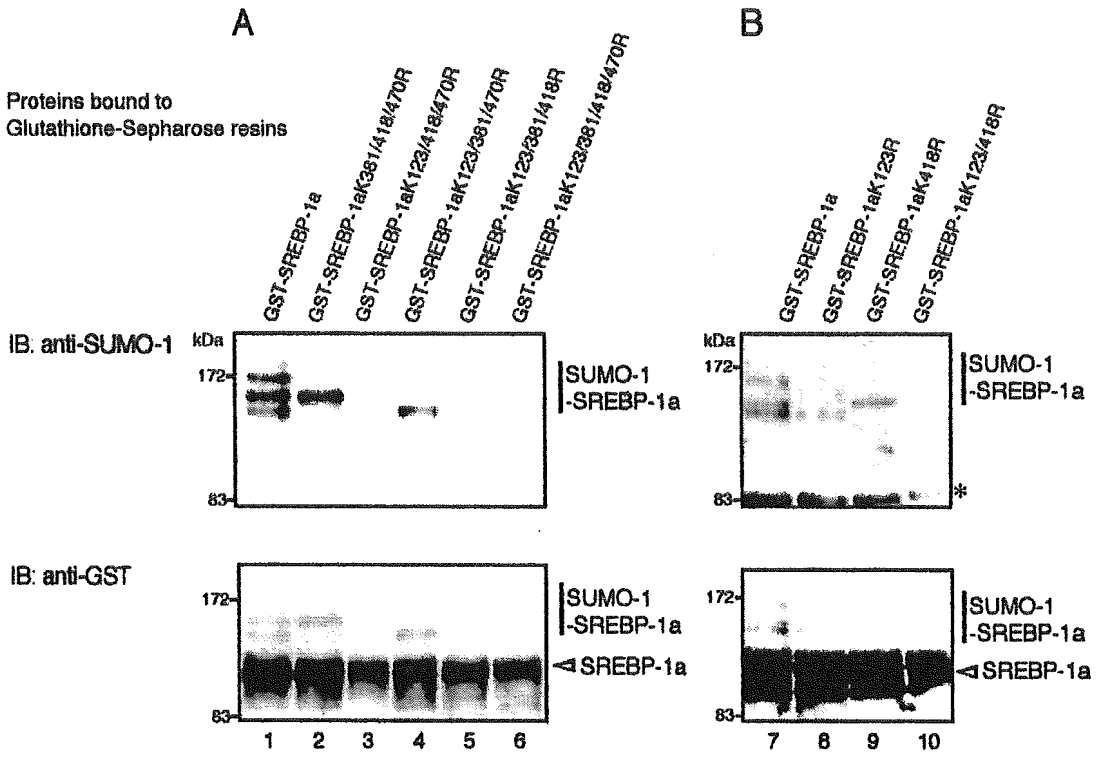

FIG. 3. **Both Lys^{123} and Lys^{123} in the nuclear form of SREBP-1a are modified by SUMO-1.** COS-1 cells were transfected with expression plasmids for His-SUMO-1 and either wild-type or mutant versions of GST-SREBP-1a. GST fusion proteins were purified with glutathione-Sepharose resins and subjected to immunoblotting (*IB*) with anti-SUMO-1 (*top*) and SREBP-1a (*bottom*) antibodies. *A*, the cells were transfected with expression plasmids for mutant versions of GST-SREBP-1a lacking 3 or 4 lysine residues among four potential sumoylation sites. *B*, mutant versions of SREBP-1a containing one or both of two possible sumoylation sites, Lys^{123} and Lys^{418}, were expressed in the cells. The mobilities of the SUMO-1-modified and -unmodified SREBP-1a are indicated on the *right*. An *asterisk* marks the nonspecific bands observed in all lanes.

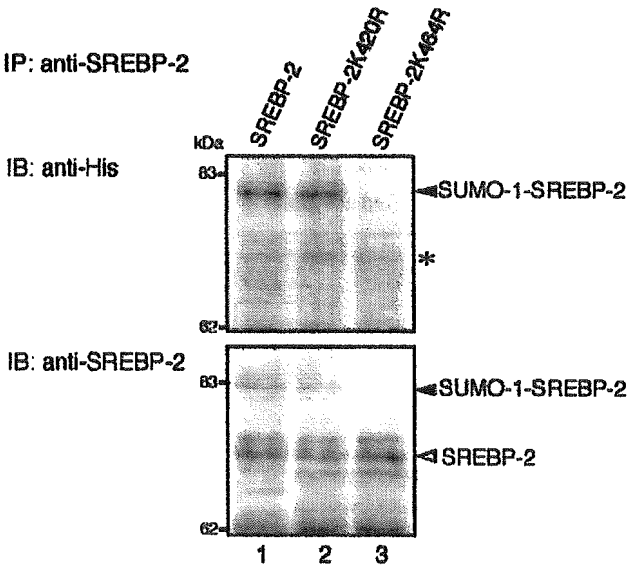

FIG. 4. **Lys^{464} is the sumoylation site in the nuclear form of SREBP-2.** COS-1 cells were cotransfected with expression plasmids for His-SUMO-1 and either wild-type or mutant versions (K420R and K464R) of SREBP-2. After 48 h of culture, immunoprecipitates (*IP*) with anti-SREBP-2 antibodies were subjected to immunoblotting (*IB*) with anti-RGS(H)$_4$ (*top*) and SREBP-2 (*bottom*) antibodies as described in the legend to Fig. 1. The mobilities of the SUMO-1-modified and -unmodified SREBP-2 are indicated on the *right*.

mutant versions of SREBPs. The cells were cultured under the sterol-loaded condition to suppress the processing of endogenous SREBPs, and luciferase assays were carried out. As shown in Fig. 5*A*, both SREBP-1aK123R and -K418R significantly increased luciferase activities compared with wild-type SREBP-1a. Double mutation markedly activated the transcription of the reporter gene. Fig. 5*B* also shows that SREBP-2K464R markedly activated transcription of the reporter gene compared with wild-type SREBP-2. Similar results were obtained using a reporter plasmid containing the promoter region of the human HMG-CoA synthase gene (data not shown). These results indicate that sumoylation of both SREBP-1a and SREBP-2 negatively regulates their transcriptional activities and that sumoylation at both Lys^{123} and Lys^{418} of SREBP-1a coordinately attenuates the transcription.

SREBPs require co-regulatory transcription factors, such as Sp1 and CBF/NF-Y, that bind DNA sequences adjacent to the SREBP binding sites and enhance the transcriptional activities of SREBPs by forming complexes with SREBPs (33, 41). Based on these early findings, we speculated that sumoylation might influence the interaction between SREBPs and these co-regulatory factors. Alternatively, it is possible that modification by SUMO-1 may weaken the affinity between SREBPs and their responsive DNA sequences. Instead of focusing on these possibilities, we evaluated whether sumoylation of SREBPs directly resulted in inactivation of these proteins. Accordingly, we used the heterologous Gal4 system with a reporter plasmid, pG5Luc. In this assay the luciferase gene transcription is driven by a promoter that contains five consensus Gal4-binding sites, without any co-regulatory transcription factors. Sumoylated SREBPs were shown in the *insets* in Fig. 5, *C* and *D*. The mutations at Lys^{123} and Lys^{418} resulted in a 1.9- and 2.1-fold increase in luciferase activities compared with Gal4-SREBP-1a, respectively (Fig. 5*C*). Furthermore, Gal4-SREBP-1aK123R/K418R, which was no longer sumoylated (Fig. 5*C*, *inset*), was more potent than Gal4-SREBP-1aK123R and -K418R. Fig. 5*D* also